

The guanine nucleotide exchange factor Arhgef5 plays crucial roles in Src-induced podosome formation

Miho Kuroiwa, Chitose Oneyama, Shigeyuki Nada and Masato Okada*

Department of Oncogene Research, Research Institute for Microbial Diseases, Osaka University, 3-1 Yamadaoka, Suita, Osaka 565-0871, Japan

*Author for correspondence (okadam@biken.osaka-u.ac.jp)

Accepted 19 January 2011

Journal of Cell Science 124, 1726-1738

© 2011. Published by The Company of Biologists Ltd

doi:10.1242/jcs.080291

Summary

Podosomes and invadopodia are actin-rich membrane protrusions that play a crucial role in cell adhesion and migration, and extracellular matrix remodeling in normal and cancer cells. The formation of podosomes and invadopodia is promoted by upregulation of some oncogenic molecules and is closely related to the invasive potential of cancer cells. However, the molecular mechanisms underlying the podosome and invadopodium formation still remain unclear. Here, we show that a guanine nucleotide exchange factor (GEF) for Rho family GTPases (Arhgef5) is crucial for Src-induced podosome formation. Using an inducible system for Src activation, we found that Src-induced podosome formation depends upon the Src SH3 domain, and identified Arhgef5 as a Src SH3-binding protein. RNA interference (RNAi)-mediated depletion of Arhgef5 caused robust inhibition of Src-dependent podosome formation. Overexpression of Arhgef5 promoted actin stress fiber remodeling through activating RhoA, and the activation of RhoA or Cdc42 was required for Src-induced podosome formation. Arhgef5 was tyrosine-phosphorylated by Src and bound to Src to positively regulate its activity. Furthermore, the pleckstrin homology (PH) domain of Arhgef5 was required for podosome formation, and Arhgef5 formed a ternary complex with Src and phosphoinositide 3-kinase when Src and/or Arhgef5 were upregulated. These findings provide novel insights into the molecular mechanisms of podosome and invadopodium formation induced by Src upregulation.

Key words: Podosome, Invadopodium, Src, Guanine nucleotide exchange factor (GEF), SH3 domain

Introduction

Invasion is one of the most characteristic features of cancer malignancy. Cancer invasion is the process in which tumor cells degrade the adjacent extracellular matrix (ECM) and migrate into surrounding tissues. Accumulating evidence suggests that the cancer invasion depends upon invadopodia (Chen, 1989; Monsky et al., 1994). Invadopodia are actin-rich membrane protrusions associated with high levels of proteases that degrade ECM. They form on the ventral surface of the plasma membrane that is perpendicular to and in contact with the ECM (Bowden et al., 1999; Oikawa et al., 2008). The structural and morphological features of invadopodia are similar to those of podosomes, which are actin-rich ECM-degrading membrane protrusions seen in osteoclasts, macrophages, smooth muscle cells and Src-transformed cells (Davies and Stossel, 1977; Kaverina et al., 2003; Tarone et al., 1985; Zamboni-Zallone et al., 1988). Despite their physiological and pathological importance, the mechanisms underlying podosome and invadopodium formation still need to be clarified.

The Src family kinases (SFKs) are non-receptor tyrosine kinases, which were originally identified as proto-oncogene products (Hunter and Sefton, 1980; Jove and Hanafusa, 1987). They play pivotal roles in various signaling pathways involved in cell growth, differentiation, adhesion, migration, invasion and metastasis (Brown and Cooper, 1996). In a wide variety of cancers, especially in mammary carcinoma, colon cancer, prostate cancer and squamous cell carcinomas, Src is often overexpressed and activated, which implies that it plays a role in cancer malignancy (Cartwright et al., 1989; Chang et al., 2007; Lehrer et al., 1989; van Oijen et al., 1998). A recent expression profiling strategy revealed that the expression level of Src correlates with poor prognosis in cancer (Aligayer et al., 2002; Creighton, 2008). Activation of Src is also

essential for the formation and function of podosomes (Erikson et al., 1980; Frame, 2004; Miyazaki et al., 2004). Furthermore, *Src*-knockout mice develop severe osteopetrosis as a result of defective podosome formation in osteoclasts (Tiffée et al., 1999). These lines of evidence suggest that Src contributes to cancer malignancy, including both invasion and metastasis, by upregulating podosome and invadopodium formation and function. However, the underlying molecular mechanism regulating these events remains elusive.

Podosomes and invadopodia are associated with a multi-protein complex consisting of adhesion molecules, actin-modulating proteins, tyrosine kinases and matrix metalloproteinases (MMPs) (Chan et al., 2009; Luxenburg et al., 2006a; Yamaguchi et al., 2005). The compositions of this complex are similar to those associated with focal adhesions (FAs), although there are apparent differences in their ECM-degrading activity and how they associate with stress fibers. Stress fibers are disrupted in cells with podosomes and invadopodia, whereas FAs associate and assemble with stress fibers (Carragher and Frame, 2004; Gimona and Buccione, 2006; Schoenwaelder and Burridge, 1999). Furthermore, podosomes and invadopodia specifically contain cortactin, N-WASP and Tks5 (also known as Fish), all of which can serve as substrates for Src family kinases (Mizutani et al., 2002; Oser et al., 2009; Seals et al., 2005; Suetsugu et al., 2002). Cortactin and N-WASP are required for actin remodeling during invadopodium formation (Luxenburg et al., 2006b; Mizutani et al., 2002; Yamaguchi et al., 2005). Tks5 localizes specifically to podosomes through its Phox homology (PX) domain, which associates with phosphatidylinositol 3-phosphate and phosphatidylinositol (3,4)-bisphosphate [PtdIns(3)P and PtdIns(3,4)P₂] (Seals et al., 2005). Because PtdIns(3,4)P₂ is highly concentrated within podosomes (Oikawa et al., 2008), production of PtdIns(3,4)P₂ might be necessary for the assembly

of crucial molecules in the podosomes. Recently, Oikawa et al. proposed a sequential mechanism for podosome formation (Oikawa et al., 2008): podosome formation is initiated at FAs owing to changes in the phosphorylation status of FA proteins and in the composition of phosphoinositides on the plasma membrane; the onset of actin polymerization is then triggered by Tks5 recruitment and subsequent N-WASP accumulation, which requires Tks5 to interact with both phosphoinositides and Grb2. In this mechanism, phosphoinositide 3-kinase (PI3K) plays an essential role (Oikawa et al., 2008).

Rho family small GTPases, such as RhoA, Rac1 and Cdc42, are also important for podosome formation (Berdeaux et al., 2004; Chellaiah, 2006). They are involved in podosome formation by regulating the actin cytoskeleton, which is under the control of a variety of guanine nucleotide exchange factors (GEFs), including the Dbl family (Quilliam et al., 1995; Rossman et al., 2005; Schmidt and Hall, 2002). However, it remains unclear which types of GEFs are necessary for regulating of podosome formation and how these GEFs are regulated by the upstream triggering factors, such as Src.

Most studies on Src-induced podosome formation have been performed with viral Src (*v-Src*) or a Src mutant lacking the negative regulatory site (Irby and Yeatman, 2000). However, the *SRC* gene is rarely mutated in human cancers (Biscardi et al., 2000; Irby et al., 1997; Ishizawa and Parsons, 2004; Oneyama et al., 2008) and the structure and function of the oncogenic forms of Src significantly differ from those of Src (Oneyama et al., 2008). Therefore, to elucidate the precise function of Src in podosome formation, it is necessary to evaluate the function of the activated Src. For this purpose, we developed an experimental system using a recombinant Src that was fused to a modified ligand-binding domain from the estrogen receptor (Src-MER), which could be conditionally activated by the treatment with 4-OH-tamoxifen (4-OHT). This system enabled us to analyze the initial intracellular events evoked by the activation of Src. In this system, we found that the Src-induced podosome formation depends upon the Src SH3 domain. Analysis of the proteins that bound to the Src SH3 domain revealed that a GEF for Rho family GTPases (Arhgef5) plays key roles in Src-induced podosome formation by linking the Src and PI3K pathways in podosomes.

Results

Analysis of the initial events induced by Src activation using the Src-MER construct

To analyze the initial events induced by Src activation, we developed an inducible system for the activation of Src or Fyn using Madin-Darby canine kidney (MDCK) cells or NIH3T3 cells that stably express the Src-MER or Fyn-MER construct (Fig. 1A). The addition of 4-OHT to these cells induced the activation [phosphorylated Y418 signals (Y418-P)] of Src-MER and Fyn-MER in a time-dependent manner (Fig. 1B). To examine the effects of Src or Fyn activation on podosome formation, we scored actin-enriched dot-like structures, so called 'podosome dots', as an index of the ability of podosome formation (Fig. 1C–E). Podosome dots observed in this study were colocalized with the podosome marker cortactin (Fig. 1C) and had ECM-degrading activity (Fig. 1D; supplementary material Movie 1), confirming that they are functionally linked to podosome formation. Using this system, we first found that Src induced formation of podosome dots more efficiently than Fyn (Fig. 1C,E), although the activation levels of Src and Fyn were almost comparable (Fig. 1B). Consistent with this, phosphorylation

of cortactin (Y421-P) in Src-MER cells greatly increased during the formation of podosomes, whereas that in Fyn-MER cells was substantially lower (Fig. 1B). Because it is known that phosphorylation of cortactin Y421 is important for invadopodium precursor formation (Oser et al., 2009), the lower affinity of Fyn-MER for cortactin might partly explain its lower efficacy in podosome formation. We also found that the intracellular localization of Src and Fyn was appreciably different. Src-MER was distributed in the perinuclear region of cytoplasm before 4-OHT treatment but once activated it accumulated in the plasma membrane (Fig. 1F; supplementary material Fig. S1A). By contrast, Fyn-MER was constantly localized to the plasma membrane before and after 4-OHT treatment. These data suggest that Src preferentially contributes to podosome formation by interacting with some specific components that can recruit Src to the plasma membrane.

The function of the Src SH3 domain is essential for podosome formation

Src has SH2 and SH3 domains that mediate protein–protein interactions, but they only become available when the activated Src adopts an open conformation (Fig. 1A). To examine the potential contribution of these domains to Src-induced podosome formation, we generated mutant Src-MER constructs that had a substitution at a crucial residue in either the SH3 domain (Src W120A-MER) or the SH2 domain (Src R177L-MER). By expressing these constructs in MDCK cells at comparable levels (Fig. 2A), we examined their ability to form podosomes (Fig. 2B). Interestingly, we found that activation of the Src SH3 (Src W120A-MER) mutant could only moderately induce podosome formation (Fig. 2B,C). The relocation of the activated Src to the plasma membrane was also attenuated in cells expressing the Src SH3 mutant (Fig. 2B). The reduction in podosome formation caused by the Src SH3 mutant was reproduced in NIH3T3 cells (supplementary material Fig. S1B,C). By contrast, activation of the Src SH2 mutant (Src R177L-MER) induced both podosome formation and relocation of activated molecules to the plasma membrane. However, fewer podosome-dots were formed with the Src SH2 mutant than with wild-type Src (Fig. 2B,C). These results suggest that an interaction between Src and some SH3-binding proteins is necessary for podosome formation.

Arhgef5 is identified as a Src SH3 domain-binding protein

To search for potential Src SH3-interacting proteins, we performed pull-down assays with either GST–Src SH3 domain (GST-SH3) or GST–SH3 mutant (GST-SH3 W120A) in MDCK cells. The proteins that specifically bound to GST–SH3 were resolved by SDS-PAGE and subjected to LC-MS/MS analysis (Fig. 3A). More than 30 proteins were identified as potential Src SH3-binding proteins (Fig. 3B and supplementary material Fig. S2). Notably, the previously characterized components of podosomes, such as Nck, dynamin 1, N-WASP, WIRE and VASP, were identified as potential Src SH3-interacting proteins, which suggests that activated Src can interact with some components of the podosome-associated protein complex through its SH3 domain. Of the proteins identified, we focused on Arhgef5 (Fig. 3C), because it serves as a GEF for Rho family GTPases that are potentially crucial for podosome and invadopodium formation (Chellaiah, 2006; Rossman et al., 2005; Xie et al., 2005). Additionally, there remains a missing link between Src activation and the cytoskeletal remodeling that leads to podosome formation. Arhgef5 is a member of the Dbl family of GEFs (Whitehead et al., 1997). It has a Dbl homology (DH)

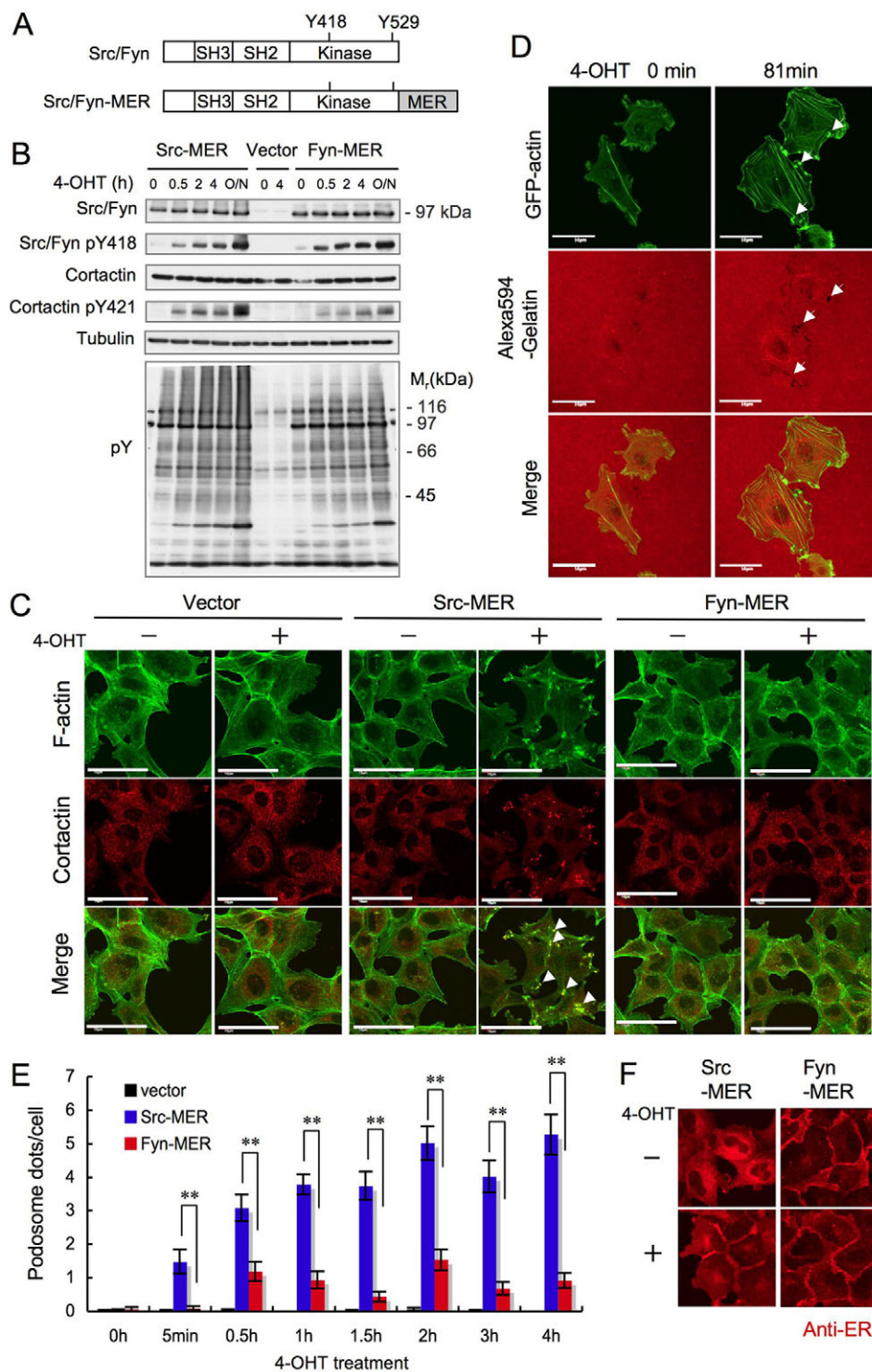


Fig. 1. Conditional activation of Src-MER induces podosome formation. (A) Schematic structures of Src and Fyn, and Src-MER and Fyn-MER. SH3, Src homology domain 3; SH2, Src homology domain 2; Kinase, kinase domain; MER, modified estrogen receptor; Y418, an autophosphorylation site; Y529, a negative regulatory site. (B) MDCK cells expressing the Src-MER or Fyn-MER construct were treated with 4-OHT (200 nM) for the indicated periods, and the total cell lysates were immunoblotted for the indicated proteins. (C) MDCK cells expressing the indicated constructs were treated with 4-OHT or ethanol for 4 hours, and stained with Alexa-Fluor-488-phalloidin (F-actin, green) or anti-cortactin antibody (red). Arrowheads indicate podosome dots. (D) NIH3T3 cells stably expressing Src-MER were transfected with GFP-actin and cultured on Alexa-Fluor-594-gelatin-coated glass coverslips overnight. The podosome formation and degradation of gelatin were observed by time-lapse analysis that started after the addition of 4-OHT (supplementary material Movie 1). Images at the time points of 0 min and 81 minutes are shown. Arrows indicate the developing podosomes. (E) MDCK cells expressing the indicated constructs were treated with 4-OHT for the indicated periods, and F-actin-positive podosome dots (Fig. 1C) were counted. The mean numbers (\pm s.e.m.) of podosome dots per cell were obtained from three independent experiments each with 50 cells. $**P < 0.01$, Student's *t*-test. (F) MDCK cells expressing Src-MER or Fyn-MER were treated with (+) or without (-) 4-OHT for 4 hours, and stained with anti-estrogen receptor (ER) antibody (red). Magnified views of images presented supplementary material Fig. S1A are shown. Scale bars: 50 μ m.

domain that has GEF activity, a pleckstrin homology (PH) domain that binds to phosphoinositides, and a SH3 domain in its C-terminal region (Fig. 3C). Arhgef5 has two isoforms; the short isoform, consisting of the C-terminal 519 amino acids (in humans) of Arhgef5, termed TIM, was previously identified as a potential oncogene product (Chan et al., 1994; Xie et al., 2005). In the present study, we identified a long isoform, hereafter termed Arhgef5, that encompasses the entire *Arhgef5* gene and contains a non-conserved unique domain in its N-terminal half (Fig. 3C). The

interaction between the Src SH3 domain and Arhgef5 was confirmed by a pull-down assay in NIH3T3 cells expressing FLAG-Arhgef5 (Fig. 3D). These results indicate that Arhgef5 is a member of the Src SH3-domain-binding proteins.

Arhgef5 is crucial for Src-induced podosome formation and invasive activity

To examine whether Arhgef5 is involved in Src-induced podosome formation, we performed siRNA-mediated knockdown of Arhgef5

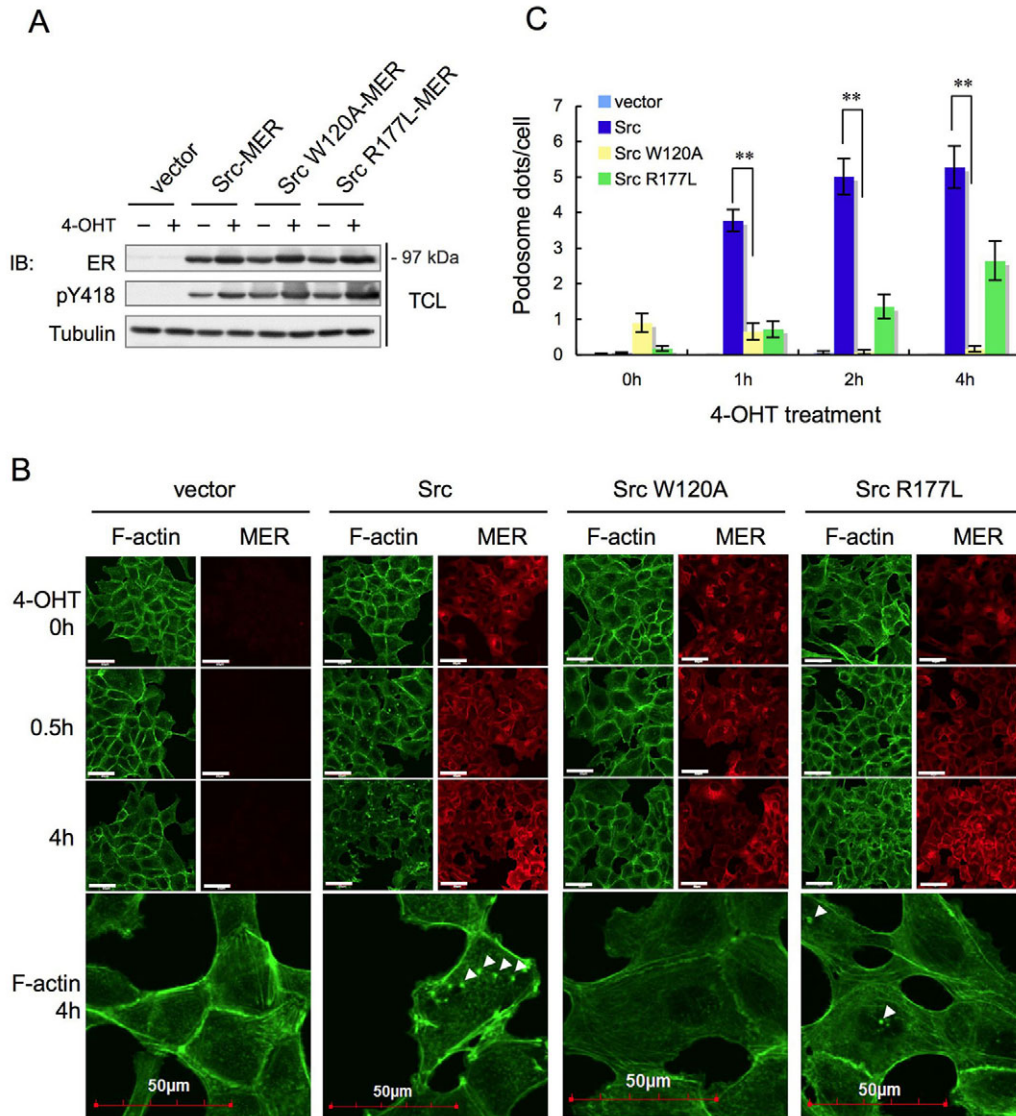


Fig. 2. The Src SH3 domain is essential for podosome formation. (A) Total cell lysates (TCL) from MDCK cells expressing Src-MER, Src W120A-MER (a SH3 mutant) or Src R177L-MER (a SH2 mutant) were immunoblotted (IB) for the indicated proteins. (B) Intracellular localization of F-actin (green, phalloidin) and Src-MER constructs (red, anti-ER antibody) in MDCK cells expressing the indicated constructs were analyzed by immunostaining. Cells were treated with 4-OHT for the indicated periods. Lower panels are magnified views of the F-actin-stained cells. Arrowheads indicate podosome dots. (C) MDCK cells expressing the indicated constructs were treated with 4-OHT for the indicated periods, and the numbers of F-actin-positive podosome dots were counted. The mean numbers (\pm s.e.m.) of podosome dots per cell were obtained from three independent experiments, each with 50 cells. ** $P < 0.01$, Student's *t*-test. Scale bars: 50 μ m.

in NIH3T3 cells expressing Src-MER. Because the expression of the short form was not detectable in NIH3T3 cells (Xie et al., 2005), we employed these cells to specifically analyze the function of the long form of Arhgef5. Depletion of Arhgef5 caused a significant reduction in podosome formation induced by Src activation (Fig. 4A–C; supplementary material Fig. S3A). The expression of FLAG–Arhgef5 or GFP–Arhgef5 carrying silent mutations in the Arhgef5 siRNA target sequence restored the ability of Arhgef5-knockdown cells to form podosomes (Fig. 5C, Fig. 8C). To further verify the role of Arhgef5, we examined the effects of Arhgef5 siRNA on Src-induced invasive activity, which can reflect the ability of podosome formation. A Matrigel invasion assay showed that depletion of Arhgef5 could significantly ($P < 0.01$) attenuate the invasive activity of NIH3T3 cells, in which Src-MER was activated (Fig. 4D). These observations demonstrate that Arhgef5 plays a crucial role in Src-induced podosome formation.

GEF activity of Arhgef5 is required for Src-induced podosome formation

To address the function of Arhgef5, we examined the effects of overexpression of full-length Arhgef5 (FULL) or a DH domain-

deficient mutant (Δ DH) on Src-induced podosome formation (Fig. 5A,B and supplementary material Fig. S3B). Even before 4-OHT treatment, the expression of Arhgef5 FULL induced the formation of thick stress fibers at the cell periphery and induced a small number of podosome dots. Similar effects of Arhgef5 on actin stress fibers were also observed in parental NIH3T3 cells (supplementary material Fig. S3C). These results are consistent with the previous observation that TIM regulates cytoskeletal organization in a Rho-dependent manner (Xie et al., 2005). Upon activation of Src-MER, podosome formation was appreciably promoted in these cells (Fig. 5B), and, notably, the formation of mature ‘podosome ring’ structures (Fig. 5A, magnified views) became more evident compared with that in mock-transfected cells. These results suggest that Arhgef5 can facilitate podosome maturation. By contrast, the expression of Δ DH did not affect actin stress fibers, and it robustly suppressed the Src-induced podosome formation (Fig. 5A,B), indicating that Δ DH can function as a dominant-negative form of Arhgef5. Furthermore, re-expression of Δ DH upon Arhgef5 knockdown failed to restore their ability to form podosomes (Fig. 5C). In these cells, the DH domain alone, the N-terminal unique domain and the C-terminal TIM domain did

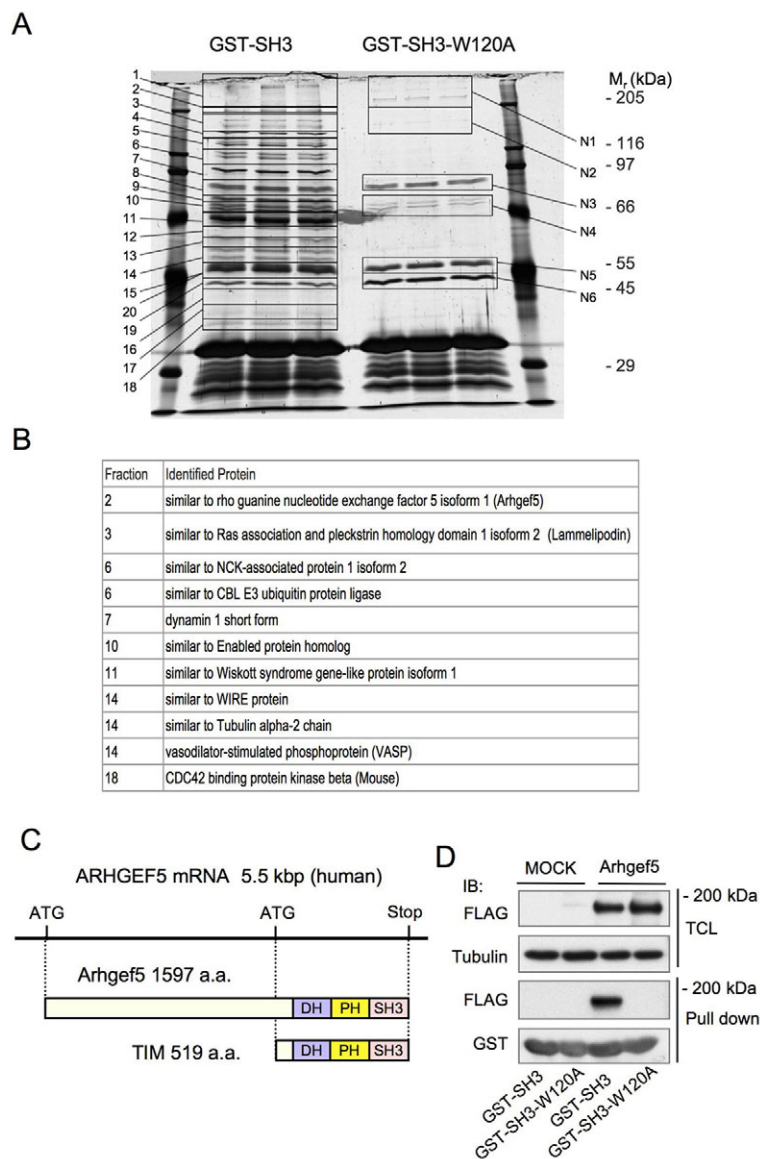


Fig. 3. Identification of Src SH3 binding proteins. (A) MDCK cells expressing Src-MER were treated with 4-OHT, and the total cell lysates were pulled down with the Src SH3 domain fused to GST (GST-SH3) or its defective mutant (GST-SH3-W120A). The bound proteins were separated by SDS-PAGE followed by silver staining. The regions indicated by numbered boxes were excised and subjected to LC-MS/MS analysis. (B) Representative proteins identified by LC-MS/MS analysis are listed. Fraction numbers correspond to the numbered boxed areas in A. Other identified proteins are listed in supplementary material Fig. S2. (C) Schematic structures of Arhgef5 and TIM proteins. DH, Dbl homology domain; PH, pleckstrin homology domain. (D) NIH3T3 Src-MER cells were transfected with 3×FLAG or Arhgef5-3×FLAG, and the total cell lysates (TCL) were immunoblotted (IB) for the indicated proteins (upper two panels). The total cell lysates were then pulled down with GST-SH3 or GST-SH3-W120A, and the bound proteins were immunoblotted for the indicated proteins (Pull down, lower two panels).

not induce podosome formation. These findings demonstrate that the GEF activity and the full-length structure of Arhgef5 are required for Src-induced podosome formation.

Previously, it was reported that TIM is a potent activator of RhoA and also exhibits activity toward Rac1 and Cdc42 *in vivo* (Xie et al., 2005). Here, we examined the specificity of full-length Arhgef5 and the effect of Src-MER activation on the activity of Rho GTPases. NIH3T3 cells expressing Src-MER and those stably overexpressing Arhgef5 FULL or Δ DH were treated with or without 4-OHT, and the active forms of Rho family GTPases were pulled down with Rhotekin-RBD- or PAK-CRIB-conjugated beads (Fig. 6A). The activation of Src-MER induced only a slight increase in the activity of RhoA in these cells (Fig. 6A). This phenomenon was consistent with the previous observation in Src-transformed cells where Src-dependent activation of total Rho cannot be detected by pull-down assays, but active Rho localized to podosomes and induced by oncogenic Src is required for their assembly and function (Berdeaux et al., 2004). The Src-dependent activation of Rac1 or Cdc42 was also not appreciable in these assays, potentially owing

to localized activation of these Rho family GTPases in the cells. However, we found that the overexpression of Arhgef5 FULL, but not Δ DH, induced a robust activation of the basal RhoA activity (Fig. 6A). By contrast, these constructs did not induce detectable activation of Rac1 or Cdc42 under the same conditions. These observations suggest that Arhgef5 can also serve as a potent activator of RhoA in these cells, although its potential contribution to the activation of Rac1 or Cdc42 cannot be excluded (Xie et al., 2005).

To confirm the contribution of Rho family GTPases to the Src-induced podosome formation, we introduced dominant-negative forms of the Rho GTPases (RhoAN19, Rac1N17 and Cdc42N17) into NIH3T3 cells expressing Src-MER and Arhgef5. The expression of RhoAN19 and Cdc42N17 almost completely suppressed Src-induced podosome formation, whereas that of Rac1N17 did not significantly affect the podosome formation (Fig. 6B,C). These results indicate that activation of RhoA is crucial to induce podosome formation through the Src-Arhgef5 pathway and that Cdc42 also plays crucial roles in pathways downstream of RhoA.

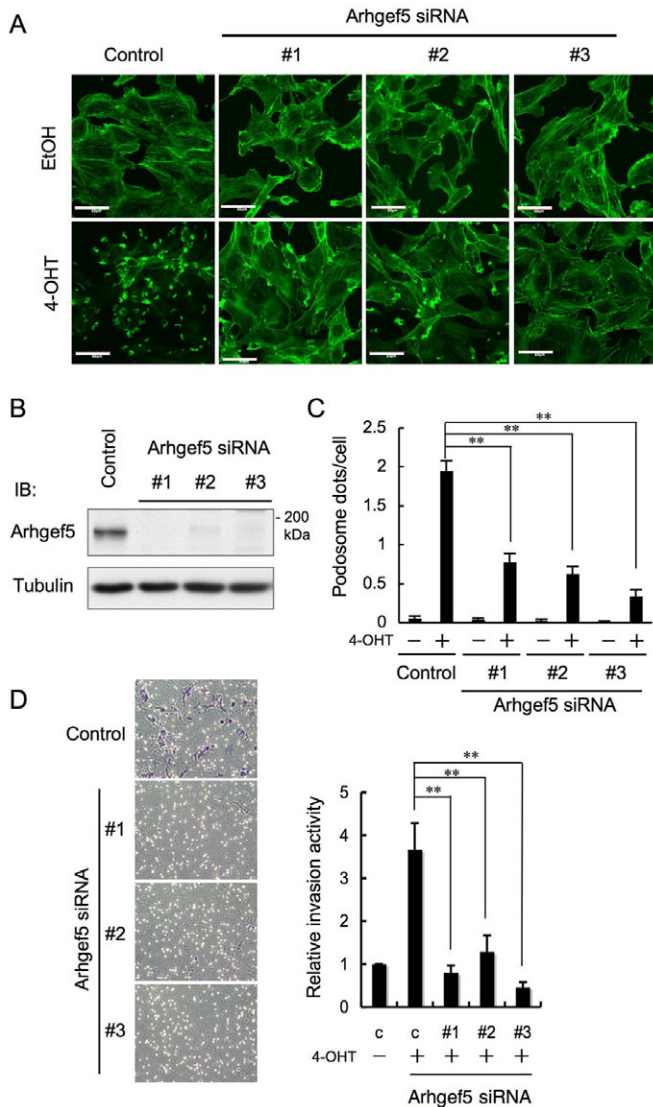


Fig. 4. Arhgef5 is crucial for podosome formation. (A) NIH3T3 Src-MER cells were transfected with control siRNA and Arhgef5 siRNA (no. 1, no. 2 or no. 3) and treated with ethanol or 4-OHT for 4 hours. The cells were stained for F-actin with Alexa-Fluor-488-phalloidin. (B) NIH3T3 Src-MER cells were treated with the indicated siRNA, and the total cell lysates were immunoblotted (IB) with anti-Arhgef5 and anti-tubulin antibodies. (C) F-actin-positive podosome dots observed in the 4-OHT-treated cells were counted. The mean numbers (\pm s.e.m.) of podosome dots per cell were obtained from three independent experiments each with 50 cells. $**P < 0.01$, Student's *t*-test. (D) The invasive activity of the cells treated with Arhgef5 siRNA was assessed by Matrigel assay. Cells were treated with 4-OHT before plating on Matrigel and were cultured for 4 hours. Invading cells were stained with Toluidine Blue. The left-hand panels show phase-contrast micrographs of invading cells. Numbers of the invading cells were counted, and the relative numbers of invading cells to cells treated with control siRNA are shown (right-hand panel). The mean numbers (\pm s.e.m.) of invading cells were obtained from three independent experiments, each with 50 cells. $**P < 0.01$, Student's *t*-test. Scale bars: 50 μ m.

Interaction between Src and Arhgef5

To elucidate the functional link between Src and Arhgef5, we examined the physical interaction between Src and Arhgef5 by immunoprecipitation assays in NIH3T3 Src-MER cells

overexpressing Arhgef5. Immunoblot analysis revealed that both the tyrosine phosphorylation of Arhgef5 and the interaction between Arhgef5 and Src were greatly increased in response to Src activation (Fig. 7A). Interestingly, we also found that the expression of Arhgef5 alone induced activation of both Src-MER and endogenous Src, and that the 4-OHT treatment further activated Src in a synergistic manner (Fig. 7B). Consistent with this finding, the tyrosine phosphorylation of total cellular proteins was enhanced by the expression of Arhgef5. However, the expression of Arhgef5 Δ DH mutant failed to induce synergistic effects on Src activity (Fig. 7C). These results indicate that the interaction between Src and Arhgef5 can further facilitate Src activation, potentially through its GEF activity, and suggest that Arhgef5 provides a platform for positive-feedback mechanism of Src regulation. The synergistic effect of Arhgef5 on Src activation was also seen in a colony formation assay in soft agar (supplementary material Fig. S4). The activation of Src-MER in mouse embryonic fibroblasts (MEFs) induced colony formation, although its efficiency was much lower than with constitutively active form of Src, SrcYF. The expression of Arhgef5 in these cells greatly enhanced the colony formation activity induced by Src activation (supplementary material Fig. S4B).

The Arhgef5 PH domain is essential for podosome formation

Phosphoinositide metabolism is important in the initiation of podosome formation (Oikawa et al., 2008). We thus speculated that the PH domain of Arhgef5 could play a role in podosome formation by targeting phosphoinositides. To address this possibility, we examined the effects of expressing the Arhgef5 PH domain (Arhgef5 PH) on Src-induced podosome formation. Immunofluorescence analysis showed that Arhgef5 PH localized to podosome dots or rings when they successfully formed (Fig. 8A, middle panels), which suggests that the Arhgef5 PH domain could potentially induce podosomes. However, on the basis of overall observation of the transfected cells, it seems more likely that the expression of Arhgef5 PH inhibited formation of podosome dots (Fig. 8A,B). These findings indicate that the Arhgef5 PH domain inhibits podosome formation by competing with the functional Arhgef5 in podosomes.

To verify the role of the Arhgef5 PH domain, we performed a restoration assay in Arhgef5-siRNA-treated cells. An RNAi-resistant form of full-length Arhgef5 (Arhgef5 FULL), a PH domain-deficient mutant (Arhgef5 Δ PH) and the PH domain alone (Arhgef5 PH) were expressed as GFP fusions proteins in these cells (Fig. 8C). Arhgef5 FULL restored the ability to form podosomes, whereas the expression of Arhgef5 Δ PH and Arhgef5 PH failed to induce podosome formation (Fig. 8D). Of note, a proportion of the FULL Arhgef5 protein was colocalized with podosome dots (Fig. 8C; supplementary material Fig. S5A). These results suggest that the PH-domain-mediated targeting of Arhgef5 to podosome precursors is required to induce podosome formation. However, in Arhgef5-knockdown cells that have no podosomes, the PH domain was highly concentrated in some endosome-like organelles, whereas Arhgef5 FULL was more widely distributed to the cell membrane and cytoplasm outside of podosomes. This indicates that the PH domain is required for podosome targeting and Arhgef5 function, but it is not sufficient to determine the precise intracellular localization of Arhgef5.

The function of Arhgef5 PH domain was examined further by a phosphoinositide array analysis using the GST-Arhgef5 PH protein.

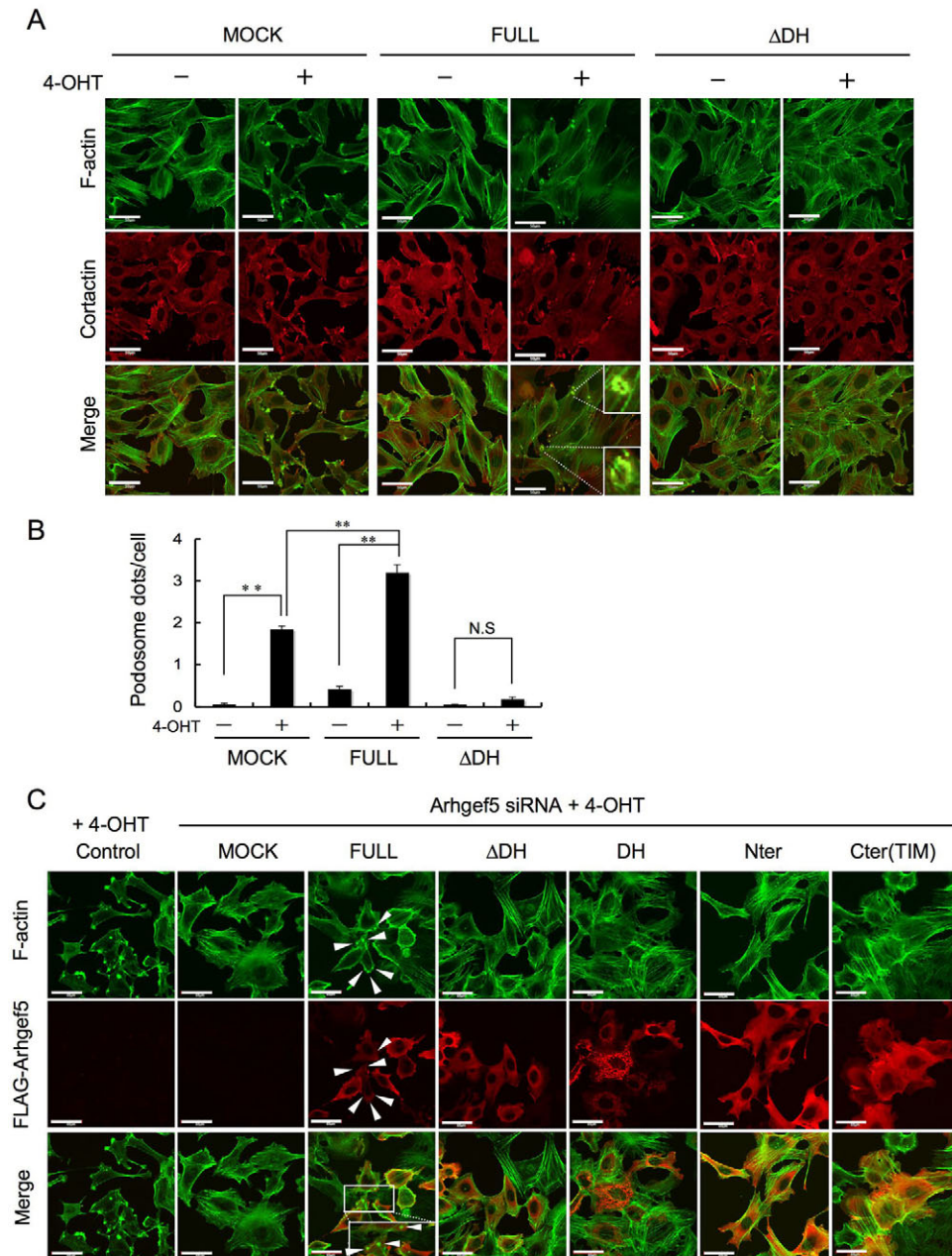


Fig. 5. GEF activity of Arhgef5 is required for Src-induced podosome formation.

(A) NIH3T3-Src-MER cells stably expressing full-length Arhgef5 (FULL) or a mutant that lacks the DH domain (Δ DH) were treated with ethanol or 4-OHT for 4 hours. The cells were stained with Alexa-Fluor-488-phalloidin (F-actin, green) and anti-cortactin antibody (red). Insets are magnified views of podosome ring-like structures. (B) F-actin-positive podosome dots observed in A were scored. The mean numbers (\pm s.e.m.) of podosome dots per cell were obtained from three independent experiments, each with 50 cells. ** $P < 0.01$, Student's *t*-test. (C) NIH3T3-Src MER cells were treated with control siRNA or Arhgef5 siRNA no. 3, and then transfected with the indicated Arhgef5 constructs. The cells were treated with 4-OHT for 4 hours, and were stained with Alexa-Fluor-488-phalloidin (F-actin, green) and anti-FLAG antibody (red). Arrowheads indicate podosome dots. A magnified view of podosome dots is shown in the inset. Scale bars: 50 μ m.

The analysis showed that Arhgef5 PH bound strongly to PtdIns(3)*P*, PtdIns(4)*P* and PtdIns(5)*P*, and weakly to PtdIns(3,4)*P*₂, PtdIns(3,5)*P*₂, PtdIns(4,5)*P*₂ and PtdIns(3,4,5)*P*₃ (supplementary material Fig. S5A). The co-sedimentation assay using liposomes also showed that Arhgef5 PH can bind various phosphoinositides with a weak preference for PtdIns(3)*P* and PtdIns(3,4)*P*₂ (supplementary material Fig. S5B). These observations suggest that Arhgef5 PH domain can recognize a wide array of phosphoinositides, and the specificity is determined by combination with other domains, such as the N-terminal unique domain and the DH domain.

Arhgef5 forms a complex with Src and PI3K

A previous study showed that PI3K is crucial for podosome formation (Nakahara et al., 2003). Consistent with this study, the inhibition of PI3K with LY294002 effectively suppressed the Src-

induced podosome formation (supplementary material Fig. S6). Furthermore, it is well established that PI3K is activated downstream of Src, and that the p85 subunit of PI3K serves as both a substrate and a binding partner of Src. On the basis of these lines of evidence, we examined the relationship between Arhgef5, Src and PI3K.

In immunoprecipitation assays using NIH3T3 Src-MER cells expressing Arhgef5 FULL, Arhgef5 Δ PH or Arhgef5 PH, we found that Arhgef5 FULL and Arhgef5 Δ PH could form a ternary complex with Src and PI3K, and that complex formation was enhanced by the activation of Src (Fig. 9A). Tyrosine phosphorylation of Arhgef5 Δ PH was also enhanced by Src activation in a manner similar to that of Arhgef5 FULL phosphorylation. These findings indicate that the PH domain is not involved in complex formation or Arhgef5 phosphorylation, and that these events occur irrespective of phosphoinositide accumulation in podosomes. The *in vitro*

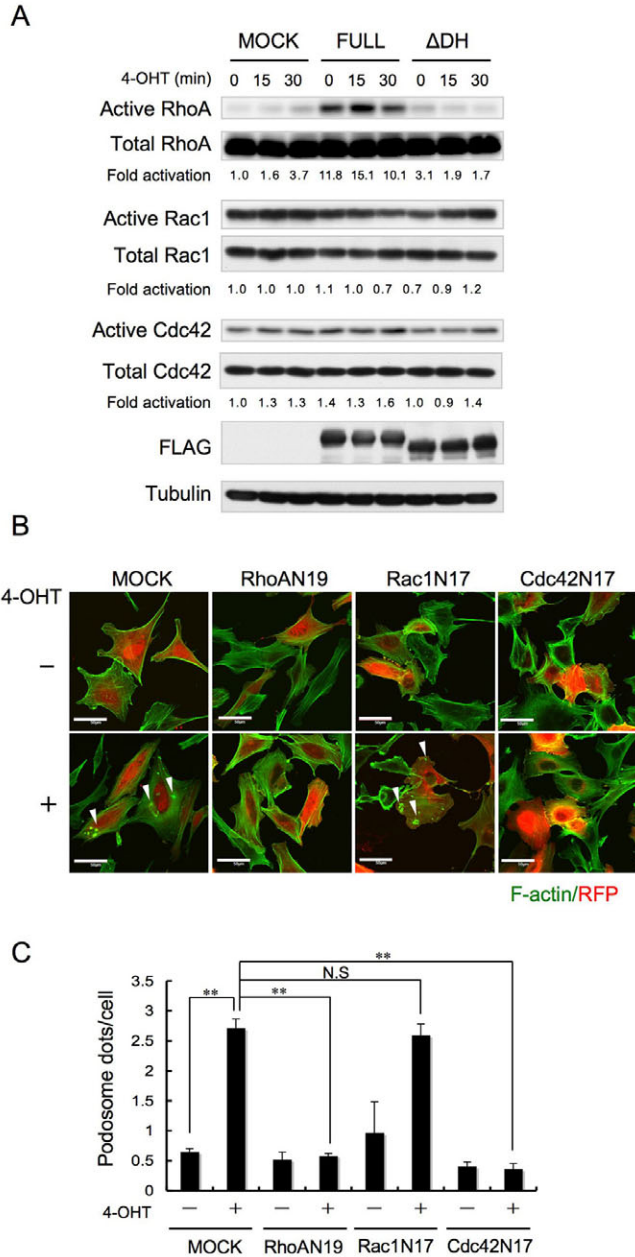


Fig. 6. GEF activity toward RhoA is important for Src-induced podosome formation. (A) NIH3T3-Src-MER cells expressing 3×FLAG (MOCK), Arhgef5-3×FLAG (FULL) or Arhgef5 ΔDH-3×FLAG (ΔDH) were treated with 4-OHT for the indicated time, and active Rho family GTPases were pulled down from the total cell lysates with Rhotekin-RBD- or GST-PAK-CRIB-conjugated beads. Bound Rho family GTPases (Active) and total Rho family GTPases in the lysates (Total) were detected by immunoblotting. The expression of Arhgef5 and ΔDH was confirmed by immunoblotting with anti-FLAG antibody. The numbers (fold activation) show a quantification of activation by densitometry analysis, with the mock-treated cells designated as 1. The results are representative of three independent experiments. (B) NIH3T3-Src-MER cells expressing Arhgef5 were transfected with a dominant negative form of RFP-Rho GTPase (RhoAN19, Rac1N17 or Cdc42N17), and treated with (+) or without (-) 4-OHT for 4 hours. The cells were stained for F-actin (green), and the expression of Rho family GTPases was detected as RFP signals. Arrowheads indicate podosome dots or rings. (C) The podosome dots in RFP-positive cells observed in B were counted. The mean numbers (±s.e.m.) of podosome dots per cells were obtained from three independent experiments, each with 50 cells. ***P*<0.01, Student's *t*-test.

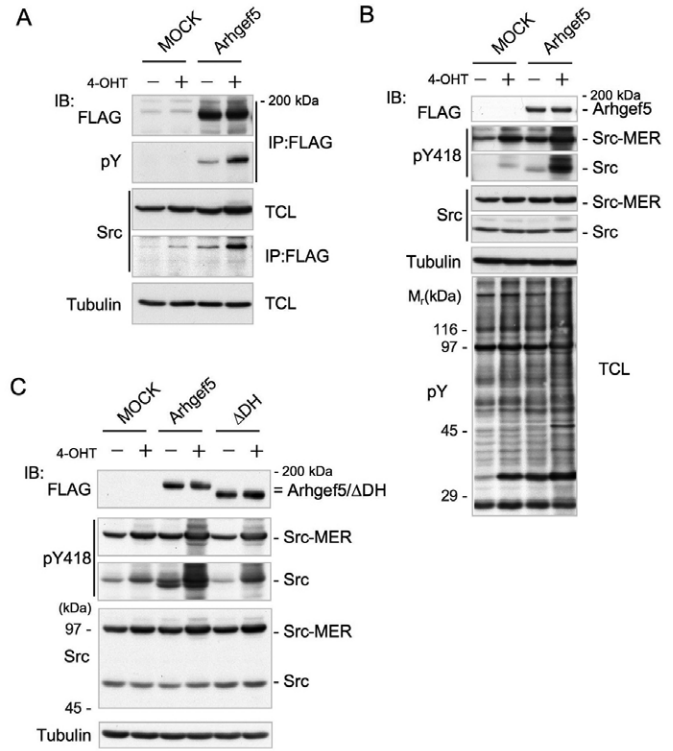


Fig. 7. Interaction between Src and Arhgef5. (A) NIH3T3-Src-MER cells expressing 3×FLAG or Arhgef5-3×FLAG were treated with (+) or without (-) 4-OHT, and the total cell lysates (TCL) were subjected to immunoprecipitation (IP) with anti-FLAG antibody followed by immunoblotting (IB) for the indicated proteins. (B) The cell lysates used in A were immunoblotted for the indicated proteins. (C) NIH3T3-Src-MER cells expressing 3×FLAG, Arhgef5-3×FLAG or Arhgef5 ΔDH-3×FLAG were treated with or without 4-OHT, and the total cell lysates were subjected to immunoblotting for the indicated proteins.

binding assays using various deletion mutants of Arhgef5 revealed that PI3K binds to a specific region (amino acids 583–902) in the N-terminal domain of Arhgef5 (supplementary material Fig. S7). The ternary complex formation was also observed previously in the highly metastatic LuM1 cells derived from murine colon adenocarcinoma 26 cells (Hyuga et al., 1994). LuM1 cells have an upregulation of Src and Arhgef5, and actively form podosomes and invadopodia in an Arhgef5-dependent manner (supplementary material Fig. S8). By contrast, the complex formation was not detectable in NM11 cells, which only show a low metastatic potential; these cells are derived from the same origin of LuM1 cells but have no upregulation of Arhgef5. This intriguing example suggests that the Arhgef5 complex is formed progressively as a consequence of upregulation of Src and Arhgef5. Taking these findings together, we propose a hypothetical model for the role of Arhgef5 in Src-induced podosome formation (Fig. 9C).

Discussion

Using an inducible Src-MER system, we addressed the molecular mechanisms underlying Src-induced podosome formation. Treating cells with 4-OHT successfully activated Src-MER, and induced podosome formation, as represented by the increased formation of podosome dots that had ECM-degrading activity. In this study, we first found that the Src SH3 domain is required for podosome

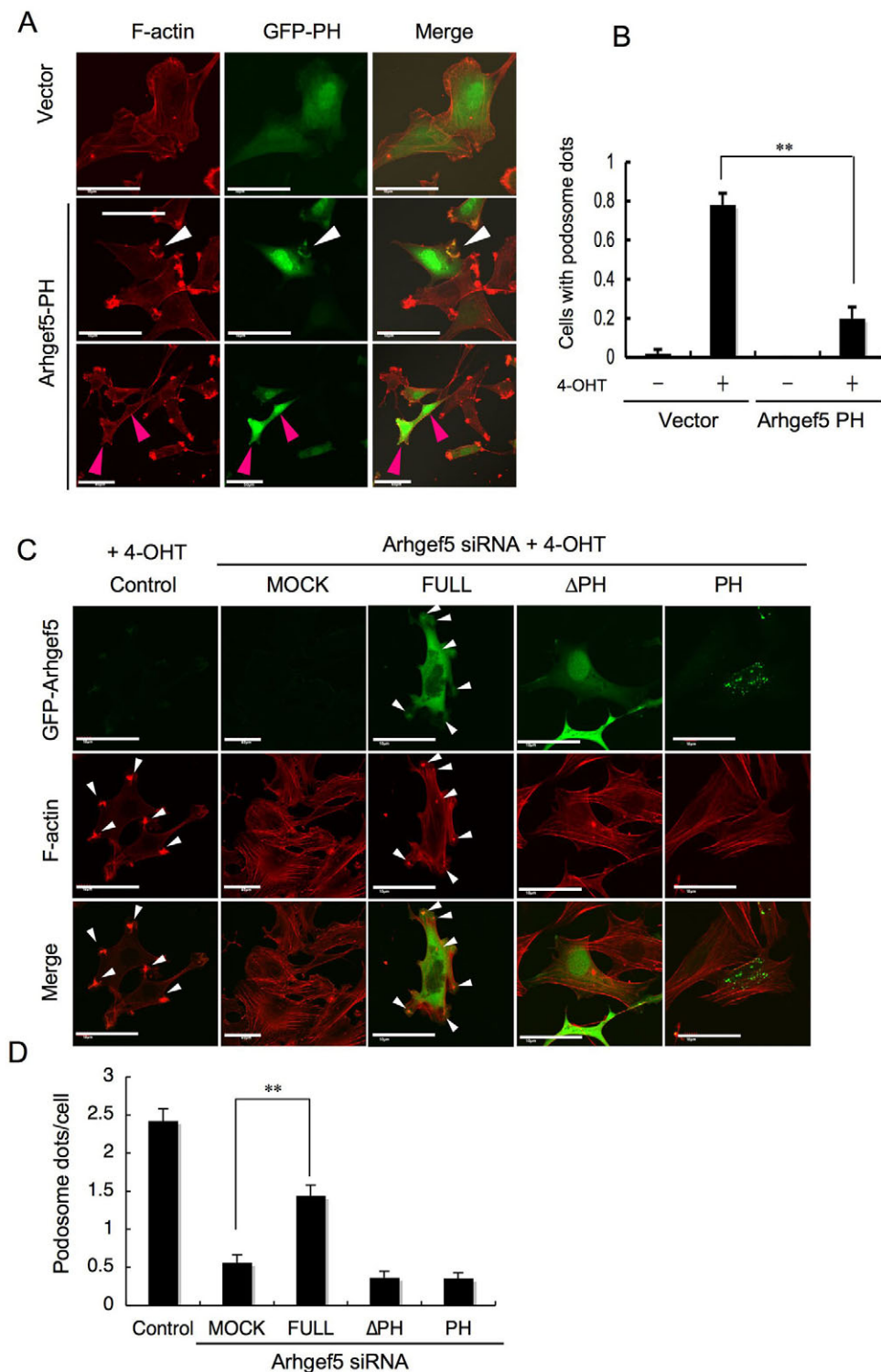


Fig. 8. Arhgef5 PH domain is essential for Src-induced podosome formation.

(A) NIH3T3-Src-MER cells were transfected with empty vector or GFP-Arhgef5 PH, and treated with 4-OHT for 4 hours. F-actin was visualized with Alexa-Fluor-594-phalloidin (red), and the location of GFP-Arhgef5 PH was observed (green). White arrowheads indicate F-actin-positive podosome dots, and pink arrowheads indicate GFP-Arhgef5-positive cells without podosomes. (B) The cells with podosome dots observed in A were counted. The mean numbers of cells (\pm s.e.m.) with podosome dots were obtained from three independent experiments, each with 100 cells. $**P < 0.01$, Student's *t*-test. (C) NIH3T3-Src-MER cells were transfected with control siRNA or Arhgef5 siRNA no. 3. After 24 hours, the cells were transfected with empty vector (MOCK), GFP-Arhgef5 FULL (FULL), GFP-Arhgef5 Δ PH (Δ PH) or GFP-Arhgef5 PH (PH), and the cells were treated with 4-OHT for 4 hours. F-actin was visualized with Alexa-Fluor-594-phalloidin (red). Arrowheads indicate F-actin positive podosome dots. (D) The podosome dots observed in C were counted. The mean numbers (\pm s.e.m.) of podosome dots per cells were obtained from three independent experiments, each with 50 cells. $**P < 0.01$, Student's *t*-test. Scale bars: 50 μ m.

formation. This proposal is consistent with previous reports showing that the binding of Tsk5 to Src SH3 plays an essential role in podosome formation (Oikawa et al., 2008; Seals et al., 2005). The crucial role of the SH3 domain in Src function was also exemplified by other previous studies using UCS15A, which is a drug that blocks SH3-mediated protein-protein interaction (Hashimoto et al., 2006; Oneyama et al., 2002; Sharma et al., 2001). On the basis of these previous studies, we decided to examine further the

function of the Src SH3 domain by identifying additional Src SH3 binding partners. Interestingly, many podosomal proteins, such as NCK, VASP, WASL and N-WASP, were included in the list of candidates, which supports the idea that Src can participate in podosome formation by functionally interacting with the podosomal protein complex.

Of the potential Src SH3 binding partners identified, we focused on Arhgef5. Arhgef5 is a potential isoform of TIM (Chan et al.,

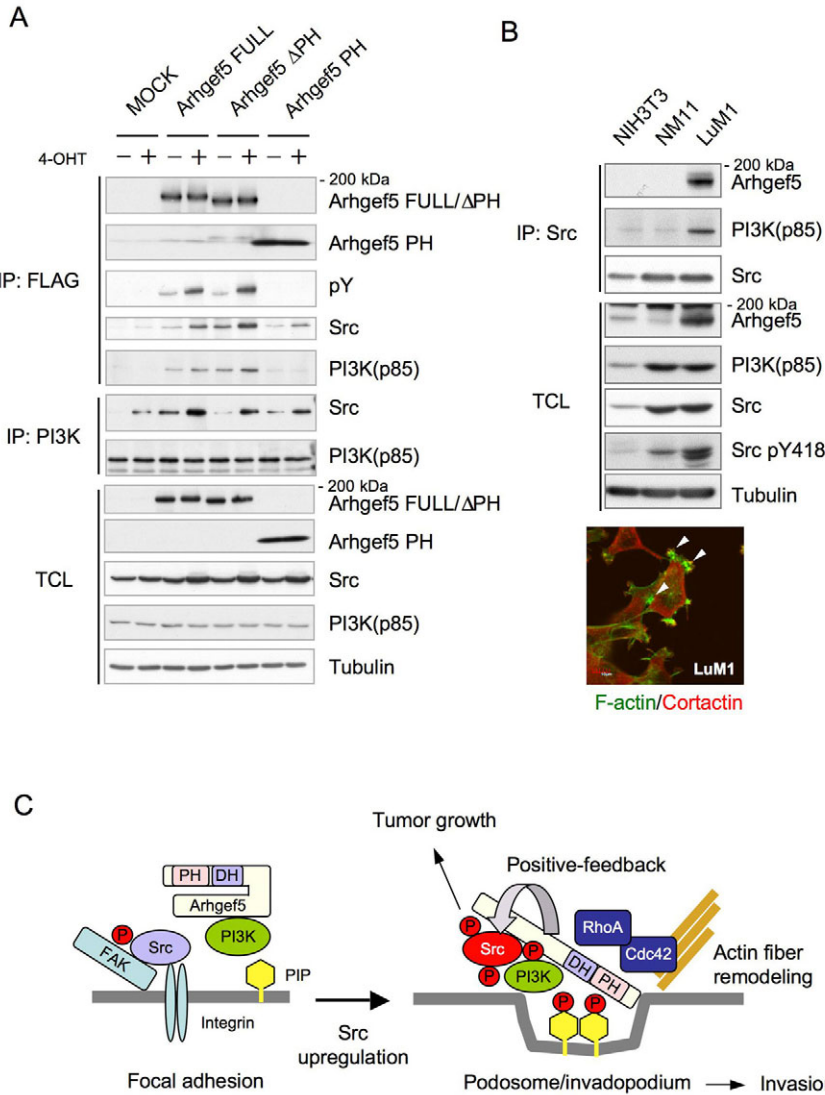


Fig. 9. Arhgef5 forms a complex with Src and PI3K independently of the PH domain. (A) NIH3T3-Src-MER cells were transfected with the indicated Arhgef5 constructs fused to 3×FLAG, and the cells were treated with or without 4-OHT for 4 hours. Total cell lysates (TCL) and the immunoprecipitates (IP) with anti-FLAG and anti-PI3K (p85) antibody were immunoblotted for the indicated proteins. (B) Total cell lysates and the immunoprecipitates with anti-Src antibody from NIH3T3, NM11 and LuM1 cells were immunoblotted for the indicated proteins (upper panels). LuM1 cells were stained for F-actin (green) and cortactin (red). Arrowheads indicate podosome and invadopodia structures. (C) A hypothetical model of the molecular mechanisms for Src-induced podosome formation. When Src is upregulated, it activates PI3K and Arhgef5 and forms a ternary complex. The complex formation further accelerates Src activation through a positive-feedback mechanism. The activated PI3K locally produce phosphoinositides, potentially at FAs, which facilitates accumulation of the Arhgef5 complex to podosomal precursors. Consequently, Arhgef5 activates RhoA and Cdc42 to assemble podosomal structures through promoting actin cytoskeletal remodeling. The activated Src in the complex might also induce tumor growth by activating downstream pathways, such as the MAPK pathway.

1996; Xie et al., 2005); however, the longer form of Arhgef5, which is a full-length product encoded by the entire *Arhgef5* gene, was completely uncharacterized. The potential oncogenic function of TIM suggested to us that it is involved in the regulation of Src-mediated podosome formation. In this study, we unveiled the following features of Arhgef5: Arhgef5 is essential for Src-induced podosome formation, Arhgef5 serves as a potent activator of RhoA to control actin cytoskeletal remodeling, Arhgef5 positively regulates Src activity, the PH domain of Arhgef5 is required for podosome formation and Arhgef5 can form a complex with Src and PI3K. These results suggest that Arhgef5 plays an important role in podosome formation by functionally linking Src, PI3K and Rho family GTPases.

We showed that Arhgef5 directly interacts with the exposed Src SH3 domain, although the binding site(s) in Arhgef5 remains unknown. An analysis using deletion mutants of Arhgef5 showed that Src SH3 could bind to various regions of Arhgef5 (data not shown). Arhgef5 has at least 12 proline-rich motifs; 11 of them are scattered throughout the N-terminal non-conserved domain, and one is in the TIM domain. These suggest that either Arhgef5 can bind to multiple Src molecules or that a higher-order structure of Arhgef5 is necessary for specific recognition by Src SH3 domain.

We found that activation of Src induced tyrosine phosphorylation of Arhgef5. This Src-dependent phosphorylation has also been reported in TIM (Yohe et al., 2008), and two tyrosine residues in the N-terminus were identified as phosphorylation sites. Phosphorylations of these residues positively regulate the GEF activity of TIM by relieving the autoinhibitory intramolecular interaction between its C-terminal SH3 domain and N-terminal polyproline region. However, Arhgef5 mutants with substitutions in the phosphorylation sites in TIM (Y1081 and/or Y1084) had no significant effect on podosome formation (data not shown). These observations suggest that the full-length Arhgef5 has additional phosphorylation sites and that it is regulated through its unique N-terminal domain in a manner distinct from TIM.

Interestingly, we noticed that the interaction between Arhgef5 and Src enhanced the activity of Src. This finding suggests that Arhgef5 itself could also be involved in the upregulation of Src function by triggering a positive-feedback loop, and that Arhgef5 functions as a scaffolding platform to stabilize, accumulate or activate Src. Moreover, we observed that Src-MER-induced anchorage-independent cell growth was appreciably enhanced by the expression of Arhgef5 (supplementary material Fig. S4B). This intriguing observation further supports the potential role of Arhgef5

as a positive regulator of Src function, although the molecular mechanism for these events must await further analysis.

A previous study showed that TIM is a potent activator of RhoA in vivo and acts as an upstream regulator for the RhoA-mediated stress fiber reorganization, although the role of TIM in podosome formation was not addressed (Xie et al., 2005). In this study, we also found that Arhgef5 could enhance formation of thick stress fibers by activating RhoA, and that inhibition of RhoA completely suppressed podosome formation. These findings suggest that the Src-Arhgef5-RhoA pathway is crucial for podosome formation. However, Cdc42 and Rac1 are also known to be involved in podosome formation by regulating actin cytoskeletal organization (Hall, 1998; Kurokawa et al., 2004). A constitutively active mutant of Cdc42 induces podosome assembly (Moreau et al., 2003), and both constitutively active and dominant-negative Cdc42 and Rac1 can disassemble podosomes (Linder et al., 1999; Ory et al., 2000). Cdc42 is one of the components of podosomes and invadopodia and functions to activate N-WASP, which induces invadopodium formation by activating the N-WASP-WIP-Arp2/3 complex (Miki and Takenawa, 2003; Yamaguchi et al., 2005). Thus, it seems that strict regulation of Cdc42 and Rac1, by their upstream regulators, is crucial for podosome organization. It has been shown that Src activates Rac1 through the Cas-Crk-DOCK180 complex and RhoA-Dial signaling (Narumiya et al., 2009). Taken together, these findings suggest that an appropriate interplay between these Rho family GTPases is involved in podosome formation and that the Src-Arhgef5-RhoA axis has a triggering role in the pathway leading to podosome formation.

We showed that the Arhgef5 PH domain is required for podosome formation, which suggests a crucial role of the interaction between the PH domain and phosphoinositides. The PH domains of Akt, Tapp and Grp have been shown to localize to podosomes and inhibit podosome formation (Furutani et al., 2006). These PH domains can bind to PtdIns(3,4) P_2 and/or PtdIns(3,4,5) P_3 , which are concentrated in podosomes (Oikawa et al., 2008). A similar inhibitory effect on podosome formation was observed for the PH domain of Arhgef5. The phosphoinositide array and liposome co-sedimentation analysis showed that the Arhgef5 PH domain was able to bind to PtdIns(3,4) P_2 and PtdIns(3,4,5) P_3 , although it had a broader binding affinity for other phosphoinositides. These results suggest that the induction of podosome formation by Arhgef5 could be mediated by its interaction with phosphoinositides. However, the intracellular distribution of Arhgef5 FULL and Arhgef5 PH was substantially different, suggesting that the PH domain is not sufficient to determine the localization of Arhgef5. An additional domain(s) or factor(s) might be necessary to direct podosomes. Consistent with a previous study (Oikawa et al., 2008), we also observed that inhibition of PI3K dramatically suppressed Src-induced podosome formation, and found that PI3K bound to a specific region of Arhgef5, forming a multi-protein complex in a manner dependent on Src activation. The formation of this complex did not depend on the PH domain of Arhgef5, which suggests that the complex forms irrespective of the recruitment of Arhgef5 to podosomes. These observations underscore the contribution of the PI3K pathway to the Src-induced podosome formation, although the underlying mechanisms need to be addressed.

On the basis of these lines of evidence, we propose a tentative mechanism for the Src-induced podosome formation (Fig. 9C). When Src is activated over a certain threshold at FAs, it interacts with Arhgef5, which in turn enhances Src activation through a

positive-feedback mechanism. The activated Src and Arhgef5 recruit PI3K, to form a ternary complex, and activates it. The activated PI3K then produces a high concentration of phosphoinositides, which directs accumulation of the Arhgef5 complex to the podosomal precursors. In the vicinity of the precursors, Arhgef5 activates RhoA, as well as Cdc42, to promote the actin cytoskeletal remodeling that is required for podosome maturation. Interestingly, we found that the Src-Arhgef5-PI3K complex was detected in highly metastatic colon adenocarcinoma LuM1 cells (Hyuga et al., 1994), but not in low metastatic NM11 cells derived from the same origin of LuM1 cells. It has also been shown that there is an upregulation of Arhgef5 in LuM1 cells but not in NM11 cells. This intriguing example suggests the potential correlation between the Arhgef5 complex formation and the invasive or metastatic ability of cancer cells. Furthermore, activated Src in the Arhgef5 complex might also activate conventional Src pathways, such as the MAPK pathway, which lead to the promotion of tumor growth (Frame, 2004). Indeed, Src-induced anchorage-independent cell growth was synergistically enhanced by the upregulation of Arhgef5. In this context, Arhgef5 might play crucial roles not only in podosome formation but also in tumor growth. To verify further the function of Arhgef5 in these pathways, studies using *Arhgef5*-knockout mice and cells, and various tumor cells, will be necessary. The elucidation of Arhgef5 function might create new opportunities for therapeutic intervention in cancer.

Materials and Methods

Reagents and antibodies

Alexa-Fluor-488-phalloidin, an Alexa-Fluor-594 protein labeling kit, and the Alexa-Fluor-594-conjugated goat anti-rabbit-IgG, anti-Src-Y418-*P*, horseradish peroxidase (HRP)-conjugated goat anti-rabbit IgG, and HRP-conjugated goat anti-mouse-IgG antibodies were purchased from Invitrogen. Anti-ER α (MC20) and anti-Src (Src2) antibodies were purchased from Santa Cruz Biotechnology. Anti-cortactin (4F11) and anti-phosphotyrosine (4G10) antibodies were obtained from Upstate Biotechnology. Anti-cortactin-Y421-*P* was purchased from Biosource. 4-Hydroxytamoxifen (H7904), LY294002, and the anti- β -tubulin (2.1), anti-GST, and anti-FLAG (M2) antibodies were from Sigma. Anti-Rac1 and anti-Cdc42 antibodies were from BD Transduction Laboratories. Anti-PI3K (p85) and anti-RhoA antibodies were from Cell Signaling Technology. Collagen type 1 was purchased from BD Biosciences. Anti-Arhgef5 antibody was generated in rabbits by immunization with GST-mouse-Arhgef5 (amino acids 2–204) and was affinity purified using maltose binding protein (MBP)-tagged antigen.

Plasmid constructs and siRNA constructs

The modified estrogen receptor (MER, amino acids 281–599) construct was a generous gift from Tohru Kimura (Osaka University, Osaka, Japan). All the constructs, including Src, Fyn and Arhgef5 (NM_133674), and their mutants, were generated by PCR using mouse cDNA as template. Src-MER, Fyn-MER, Src W120A-MER and Src R177L-MER were subcloned into the pCX4puro retrovirus vector (a gift from Tsuyoshi Akagi, KAN Research Institute, Kobe, Japan). The Src SH3 domain (amino acids 88–141) and the W120A mutant were subcloned into the pGEX6p-1 vector (GE Healthcare), and recombinant proteins were expressed in *Escherichia coli* BL21 or DH5 α . To generate a 3 \times FLAG-tagged expression vector, the 3 \times FLAG construct (Sigma) was subcloned into the pCX4brs vector. Arhgef5 Δ PH, Arhgef5 PH (amino acids 1341–1488), Arhgef5 Δ DH, Arhgef5 DH (1064–1340), Nter (amino acids 1–1063), Cter (amino acids 1064–1581) and a series of Arhgef5 fragments were subcloned into the pCX4brs-3 \times FLAG. To generate siRNA-resistant Arhgef5, the sequence for a siRNA recognition site was modified to 5'-GCCC-CACAAGAAGAGTTCAACAACACT-3' (nucleotides 2984–3010), and the silent construct was subcloned into the pCX4brs-3 \times FLAG. For immunofluorescence study, the constructs of Arhgef5 and its mutants were subcloned into the pEGFP-N1 vector (Clontech). The EGFP sequence was fused to the 3' end of Arhgef5 and its mutants, and these constructs were subcloned into pCX4brs. pEGFP-actin was obtained from Clontech. The dominant negative forms of Rho family GTPases (RhoAN19, Rac1N17 and Cdc42N17) were subcloned into pDsRed2-N1 vector (Clontech). All of the generated constructs were confirmed by sequencing. The series of Arhgef5 siRNA duplexes (Stealth, MSS225557) and Stealth siRNA Negative Control (12935-112) were purchased from Invitrogen. The siRNA sequences used are as follows: no. 1, 5'-UUCAGAGGAAGGAUCUAUGAUGAGGCC-CCUAUCAUAGAUCUUCUCUGAA-3'; no. 2, 5'-UAAGCAGUAGCAC-UUCCACUGCCUGCAGGGCAGUGGAAGUGAACUCUUA-3'; and no. 3,

5'-UGUAUUAUAAAUCUCCUGAGGGCCUCAGGAGAAUUAUAU-
AUACA-3'.

Retroviral gene transfer and transient gene transfection

The pCX4puro SFK-MER series and pCX4brs-Arhgef5 3×FLAG series of gene transfers were carried out with retroviruses. The production and infection of retroviral vectors were performed as described previously (Akagi et al., 2003). The pCX4brs-Arhgef5 GFP series was transfected with Lipofectamine LTX (Invitrogen). siRNA was introduced with Lipofectamine RNAiMAX. For the Arhgef5 restoration assay, cells transfected with siRNA were seeded onto collagen-I-coated glass coverslips and incubated for 18–24 hours before cDNA transfection. After 18 to 24 hours, cells were subjected to 4-OHT treatment and immunofluorescence observation. cDNA and siRNA transfection were performed according to the manufacturer's instructions (Invitrogen). MDCK, NIH3T3 and the ecotropic retrovirus packaging cell line Plat-E were cultured in Dulbecco's modified Eagle's medium (DMEM) supplemented with 10% fetal bovine serum (FBS). NM11 and LuM1 cells (gifts from Keizo Takenaga, Shimane University, Izumo, Japan) were cultured in RPMI 1640 medium supplemented with 10% FBS.

Immunofluorescence and fluorescent gelatin degradation assay

For immunofluorescence study, glass coverslips were coated with collagen type 1 (BD Biosciences) according to the manufacturer's instructions. For the fluorescent gelatin degradation assay, Alexa-Fluor-594-gelatin-coated dishes were prepared as described previously (Yamaguchi et al., 2010). Confocal images were obtained using a confocal laser scanning microscopy (Olympus, FV-1000).

Immunoblotting and immunoprecipitation assay

Cells were lysed in buffer (20 mM Tris-HCl pH 7.4, 150 mM NaCl, 0.5 mM EDTA, 2% ODG, 1% NP40, 10% glycerol, 10 µg/ml aprotinin, 10 µg/ml leupeptin, 1 mM PMSF, 1 mM sodium orthovanadate, 50 mM NaF and 5 mM 2-mercaptoethanol) on ice and clarified by centrifugation. Immunoblotting of cell lysates was performed as previously described (Kotani et al., 2007). Immunoprecipitation were performed as previously described (Oneyama et al., 2003). Briefly, cell lysates were quantified and equal amounts of total cell protein were immunoprecipitated overnight with the indicated antibodies (3 µg FLAG antibody and 3 µg PI3K antibody). Immunoprecipitates were collected on Protein-G-Sepharose beads (50 µl per immunoprecipitation) (GE Healthcare). Beads were washed three times in lysis buffer, and boiled in 100 µl SDS sample buffer. The protein samples were separated by SDS-PAGE, then transferred onto PVDF membranes, immunoblotted with the indicated antibodies, and subjected to chemiluminescent detection (PerkinElmer Life Sciences).

Purification of Src-SH3-domain-binding proteins

The 4-OHT-treated MDCK cells were lysed in buffer (50 mM Tris-HCl pH 7.4, 150 mM NaCl, 0.5 mM EDTA, 1% NP40, 10% glycerol, 10 µg/ml aprotinin, 10 µg/ml leupeptin, 1 mM PMSF, 1 mM sodium orthovanadate, 50 mM NaF, 5 mM 2-mercaptoethanol and 0.1% Triton X-100), and cleared by centrifugation. GST-SrcSH3 and GST-SrcSH3W120A was coupled to glutathione-Sepharose beads (GE Healthcare). The washed beads were incubated with cell lysate at 4°C for 3 hours and then collected by centrifugation. After extensive washing, the proteins recovered on the beads were eluted with 20 mM glutathione and separated by SDS-PAGE. After visualization by silver staining (Bio-Rad), protein bands were excised from the gel and digested in situ with Trypsin Gold (Promega). The digested samples were analyzed by nanocapillary reversed-phase LC-MS/MS using a C18 column on a nanoLC system (Ultimate, LC Packing) coupled to a quadruple time-of-flight mass spectrometer (QTOF Ultima, Waters) as described previously (Saito et al., 2008). Proteins were identified by database searching using Mascot Daemon (Matrix Science).

Assays of Rho family small G proteins

NIH3T3 Src-MER cells and those expressing Arhgef FULL or ΔDH were treated with 200 nM 4-OHT or ethanol for 0–30 minutes. Cells were lysed in RIPA buffer, and subjected to a pull-down assay with Rhotekin-RBD-agarose (Cell Biolabs) or GST-PAK-CRIB-bound glutathione-Sepharose, as described previously (Kurokawa et al., 2004; Yagi et al., 2007). RhoA, Rac1 and Cdc42 were detected by immunoblotting and quantified using ImageQuant LAS 4000mini (GE Healthcare).

Matrigel invasion assay

The Matrigel invasion assay was performed according to the manufacturer's instructions (BD Biosciences). Briefly, NIH3T3 Src-MER cells were transfected with control siRNA or Arhgef5 RNAi no. 1, no. 2 or no. 3 and cultured in DMEM for 35–50 hours, followed by treatment with 200 nM 4-OHT or ethanol. Then, 0.3×10^5 cells were seeded onto Matrigel Invasion Chambers (BD Biosciences). At 4 hours after seeding, cells were fixed in 100% methanol and stained with 1% Toluidine Blue. FBS (10%) was used as chemoattractant. Images of stained cells were obtained with an optical microscope (Olympus, IX-70).

We thank Tohru Kimura (Osaka University) for the kind gift of the MER construct, Tsuyoshi Akagi (KAN Research Institute) for the kind gifts of the retrovirus vectors, Michiyuki Matsuda (Kyoto University) for the kind gifts of the constructs of Rho family GTPases, Keizo Takenaga (Shimane University) for the kind gifts of NM11 and LuM1 cells, and Genki Akamatsu (Osaka University) for vector constructions of the dominant negative Rho family GTPases. We are also grateful to Mayumi Suto and Kazunobu Saito of DNA-chip Development Center for Infectious Diseases (RIMD, Osaka University) for LC-MS/MS analysis. This work was supported by a Grant-in-Aid for Scientific Research from the Ministry of Education, Culture, Sports, Science and Technology of Japan and the Uehara Memorial Foundation.

Supplementary material available online at

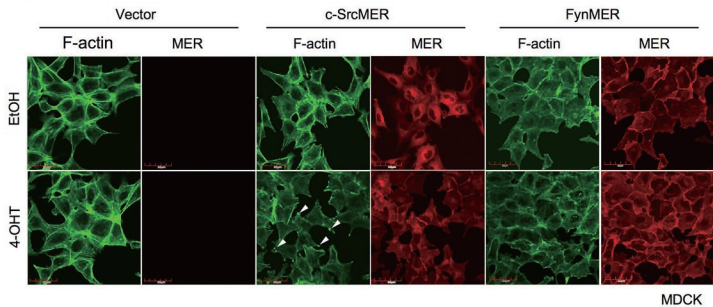
<http://jcs.biologists.org/cgi/content/full/124/10/1726/DC1>

References

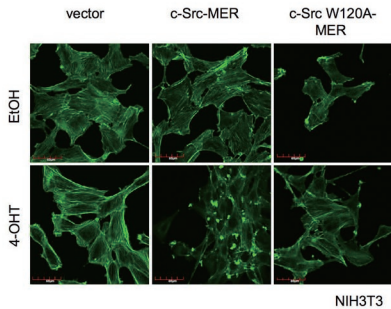
- Akagi, T., Sasai, K. and Hanafusa, H. (2003). Refractory nature of normal human diploid fibroblasts with respect to oncogene-mediated transformation. *Proc. Natl. Acad. Sci. USA* **100**, 13567–13572.
- Aligayer, H., Boyd, D. D., Heiss, M. M., Abdalla, E. K., Curley, S. A. and Gallick, G. E. (2002). Activation of Src kinase in primary colorectal carcinoma: an indicator of poor clinical prognosis. *Cancer* **94**, 344–351.
- Berdeaux, R. L., Diaz, B., Kim, L. and Martin, G. S. (2004). Active Rho is localized to podosomes induced by oncogenic Src and is required for their assembly and function. *J. Cell Biol.* **166**, 317–323.
- Biscardi, J. S., Ishizawa, R. C., Silva, C. M. and Parsons, S. J. (2000). Tyrosine kinase signalling in breast cancer: epidermal growth factor receptor and c-Src interactions in breast cancer. *Breast Cancer Res.* **2**, 203–210.
- Bowden, E. T., Barth, M., Thomas, D., Glazer, R. I. and Mueller, S. C. (1999). An invasion-related complex of cortactin, paxillin and PKCmu associates with invadopodia at sites of extracellular matrix degradation. *Oncogene* **18**, 4440–4449.
- Brown, M. T. and Cooper, J. A. (1996). Regulation, substrates and functions of src. *Biochim. Biophys. Acta* **1287**, 121–149.
- Carragher, N. O. and Frame, M. C. (2004). Focal adhesion and actin dynamics: a place where kinases and proteases meet to promote invasion. *Trends Cell Biol.* **14**, 241–249.
- Cartwright, C. A., Kamps, M. P., Meisler, A. I., Pipas, J. M. and Eckhart, W. (1989). pp60c-src activation in human colon carcinoma. *J. Clin. Invest.* **83**, 2025–2033.
- Chan, A. M., McGovern, E. S., Catalano, G., Fleming, T. P. and Miki, T. (1994). Expression cDNA cloning of a novel oncogene with sequence similarity to regulators of small GTP-binding proteins. *Oncogene* **9**, 1057–1063.
- Chan, A. M., Takai, S., Yamada, K. and Miki, T. (1996). Isolation of a novel oncogene, NET1, from neuroepithelioma cells by expression cDNA cloning. *Oncogene* **12**, 1259–1266.
- Chan, K. T., Cortesio, C. L. and Huttenlocher, A. (2009). FAK alters invadopodia and focal adhesion composition and dynamics to regulate breast cancer invasion. *J. Cell Biol.* **185**, 357–370.
- Chang, Y. M., Kung, H. J. and Evans, C. P. (2007). Nonreceptor tyrosine kinases in prostate cancer. *Neoplasia* **9**, 90–100.
- Chelliah, M. A. (2006). Regulation of podosomes by integrin alphavbeta3 and Rho GTPase-facilitated phosphoinositide signaling. *Eur. J. Cell Biol.* **85**, 311–317.
- Chen, W. T. (1989). Proteolytic activity of specialized surface protrusions formed at rosette contact sites of transformed cells. *J. Exp. Zool.* **251**, 167–185.
- Creighton, C. J. (2008). Multiple oncogenic pathway signatures show coordinate expression patterns in human prostate tumors. *PLoS ONE* **3**, e1816.
- Davies, W. A. and Stossel, T. P. (1977). Peripheral hyaline blebs (podosomes) of macrophages. *J. Cell Biol.* **75**, 941–955.
- Erikson, R. L., Purchio, A. F., Erikson, E., Collett, M. S. and Brugge, J. S. (1980). Molecular events in cells transformed by Rous Sarcoma virus. *J. Cell Biol.* **87**, 319–325.
- Frame, M. C. (2004). Newest findings on the oldest oncogene; how activated src does it. *J. Cell Sci.* **117**, 989–998.
- Furutani, M., Tsujita, K., Itoh, T., Ijuin, T. and Takenawa, T. (2006). Application of phosphoinositide-binding domains for the detection and quantification of specific phosphoinositides. *Anal. Biochem.* **355**, 8–18.
- Gimona, M. and Buccione, R. (2006). Adhesions that mediate invasion. *Int. J. Biochem. Cell Biol.* **38**, 1875–1892.
- Hall, A. (1998). Rho GTPases and the actin cytoskeleton. *Science* **279**, 509–514.
- Hashimoto, S., Hirose, M., Hashimoto, A., Morishige, M., Yamada, A., Hosaka, H., Akagi, K., Ogawa, E., Oneyama, C., Agatsuma, T. et al. (2006). Targeting AMAP1 and cortactin binding bearing an atypical src homology 3/proline interface for prevention of breast cancer invasion and metastasis. *Proc. Natl. Acad. Sci. USA* **103**, 7036–7041.
- Hunter, T. and Sefton, B. M. (1980). Transforming gene product of Rous sarcoma virus phosphorylates tyrosine. *Proc. Natl. Acad. Sci. USA* **77**, 1311–1315.
- Hyuga, S., Nishikawa, Y., Sakata, K., Tanaka, H., Yamagata, S., Sugita, K., Saga, S., Matsuyama, M. and Shimizu, S. (1994). Autocrine factor enhancing the secretion of M(r) 95,000 gelatinase (matrix metalloproteinase 9) in serum-free medium conditioned with murine metastatic colon carcinoma cells. *Cancer Res.* **54**, 3611–3616.
- Irby, R., Mao, W., Coppola, D., Jove, R., Gamero, A., Cuthbertson, D., Fujita, D. J. and Yeatman, T. J. (1997). Overexpression of normal c-Src in poorly metastatic human

- colon cancer cells enhances primary tumor growth but not metastatic potential. *Cell Growth Differ.* **8**, 1287-1295.
- Irby, R. B. and Yeatman, T. J.** (2000). Role of Src expression and activation in human cancer. *Oncogene* **19**, 5636-5642.
- Ishizawar, R. and Parsons, S. J.** (2004). c-Src and cooperating partners in human cancer. *Cancer Cell* **6**, 209-214.
- Jove, R. and Hanafusa, H.** (1987). Cell transformation by the viral src oncogene. *Annu. Rev. Cell Biol.* **3**, 31-56.
- Kaverina, I., Stradal, T. E. and Gimona, M.** (2003). Podosome formation in cultured A7r5 vascular smooth muscle cells requires Arp2/3-dependent de-novo actin polymerization at discrete microdomains. *J. Cell Sci.* **116**, 4915-4924.
- Kotani, T., Morone, N., Yuasa, S., Nada, S. and Okada, M.** (2007). Constitutive activation of neuronal Src causes aberrant dendritic morphogenesis in mouse cerebellar Purkinje cells. *Neurosci. Res.* **57**, 210-219.
- Kurokawa, K., Itoh, R. E., Yoshizaki, H., Nakamura, Y. O. and Matsuda, M.** (2004). Coactivation of Rac1 and Cdc42 at lamellipodia and membrane ruffles induced by epidermal growth factor. *Mol. Biol. Cell* **15**, 1003-1010.
- Lehrer, S., O'Shaughnessy, J., Song, H. K., Levine, E., Savoretti, P., Dalton, J., Lipsztein, R., Kalnicki, S. and Bloomer, W. D.** (1989). Activity of pp60c-src protein kinase in human breast cancer. *Mt. Sinai J. Med.* **56**, 83-85.
- Linder, S., Nelson, D., Weiss, M. and Aepfelbacher, M.** (1999). Wiskott-Aldrich syndrome protein regulates podosomes in primary human macrophages. *Proc. Natl. Acad. Sci. USA* **96**, 9648-9653.
- Luxenburg, C., Addadi, L. and Geiger, B.** (2006a). The molecular dynamics of osteoclast adhesions. *Eur. J. Cell Biol.* **85**, 203-211.
- Luxenburg, C., Parsons, J. T., Addadi, L. and Geiger, B.** (2006b). Involvement of the Src-cortactin pathway in podosome formation and turnover during polarization of cultured osteoclasts. *J. Cell Sci.* **119**, 4878-4888.
- Miki, H. and Takenawa, T.** (2003). Regulation of actin dynamics by WASP family proteins. *J. Biochem.* **134**, 309-313.
- Miyazaki, T., Sanjay, A., Neff, L., Tanaka, S., Horne, W. C. and Baron, R.** (2004). Src kinase activity is essential for osteoclast function. *J. Biol. Chem.* **279**, 17660-17666.
- Mizutani, K., Miki, H., He, H., Maruta, H. and Takenawa, T.** (2002). Essential role of neural Wiskott-Aldrich syndrome protein in podosome formation and degradation of extracellular matrix in src-transformed fibroblasts. *Cancer Res.* **62**, 669-674.
- Monsky, W. L., Lin, C. Y., Aoyama, A., Kelly, T., Akiyama, S. K., Mueller, S. C. and Chen, W. T.** (1994). A potential marker protease of invasiveness, seprase, is localized on invadopodia of human malignant melanoma cells. *Cancer Res.* **54**, 5702-5710.
- Moreau, V., Tatin, F., Varon, C. and Genot, E.** (2003). Actin can reorganize into podosomes in aortic endothelial cells, a process controlled by Cdc42 and RhoA. *Mol. Cell Biol.* **23**, 6809-6822.
- Nakahara, H., Otani, T., Sasaki, T., Miura, Y., Takai, Y. and Kogo, M.** (2003). Involvement of Cdc42 and Rac small G proteins in invadopodia formation of RPM17951 cells. *Genes Cells* **8**, 1019-1027.
- Narumiya, S., Tanji, M. and Ishizaki, T.** (2009). Rho signaling, ROCK and mDia1, in transformation, metastasis and invasion. *Cancer Metastasis Rev.* **28**, 65-76.
- Oikawa, T., Yamaguchi, H., Itoh, T., Kato, M., Ijuin, T., Yamazaki, D., Suetsugu, S. and Takenawa, T.** (2004). PtdIns(3,4,5)P₃ binding is necessary for WAVE2-induced formation of lamellipodia. *Nat. Cell Biol.* **6**, 420-426.
- Oikawa, T., Itoh, T. and Takenawa, T.** (2008). Sequential signals toward podosome formation in NIH-src cells. *J. Cell Biol.* **182**, 157-169.
- Oneyama, C., Nakano, H. and Sharma, S. V.** (2002). UCS15A, a novel small molecule, SH3 domain-mediated protein-protein interaction blocking drug. *Oncogene* **21**, 2037-2050.
- Oneyama, C., Agatsuma, T., Kanda, Y., Nakano, H., Sharma, S. V., Nakano, S., Narazaki, F. and Tatsuta, K.** (2003). Synthetic inhibitors of proline-rich ligand-mediated protein-protein interaction: potent analogs of UCS15A. *Chem. Biol.* **10**, 443-451.
- Oneyama, C., Hikita, T., Nada, S. and Okada, M.** (2008). Functional dissection of transformation by c-Src and v-Src. *Genes Cells* **13**, 1-12.
- Ory, S., Munari-Silem, Y., Fort, P. and Jurdic, P.** (2000). Rho and Rac exert antagonistic functions on spreading of macrophage-derived multinucleated cells and are not required for actin fiber formation. *J. Cell Sci.* **113**, 1177-1188.
- Oser, M., Yamaguchi, H., Mader, C. C., Bravo-Cordero, J. J., Arias, M., Chen, X., Desmarais, V., van Rheenen, J., Koleske, A. J. and Condeelis, J.** (2009). Cortactin regulates cofilin and N-WASP activities to control the stages of invadopodium assembly and maturation. *J. Cell Biol.* **186**, 571-587.
- Quilliam, L. A., Khosravi-Far, R., Huff, S. Y. and Der, C. J.** (1995). Guanine nucleotide exchange factors: activators of the Ras superfamily of proteins. *BioEssays* **17**, 395-404.
- Rossman, K. L., Der, C. J. and Sondek, J.** (2005). GEF means go: turning on RHO GTPases with guanine nucleotide-exchange factors. *Nat. Rev. Mol. Cell Biol.* **6**, 167-180.
- Saito, K., Enya, K., Oneyama, C., Hikita, T. and Okada, M.** (2008). Proteomic identification of ZO-1/2 as a novel scaffold for Src/Csk regulatory circuit. *Biochem. Biophys. Res. Commun.* **366**, 969-975.
- Schmidt, A. and Hall, A.** (2002). Guanine nucleotide exchange factors for Rho GTPases: turning on the switch. *Genes Dev.* **16**, 1587-1609.
- Schoenwaelder, S. M. and Burridge, K.** (1999). Bidirectional signaling between the cytoskeleton and integrins. *Curr. Opin. Cell Biol.* **11**, 274-286.
- Seals, D. F., Azucena, E. F., Jr, Pass, I., Tesfay, L., Gordon, R., Woodrow, M., Resau, J. H. and Courtneidge, S. A.** (2005). The adaptor protein Tks5/Fish is required for podosome formation and function, and for the protease-driven invasion of cancer cells. *Cancer Cell* **7**, 155-165.
- Sharma, S. V., Oneyama, C., Yamashita, Y., Nakano, H., Sugawara, K., Hamada, M., Kosaka, N. and Tamaoki, T.** (2001). UCS15A, a non-kinase inhibitor of Src signal transduction. *Oncogene* **20**, 2068-2079.
- Suetsugu, S., Hattori, M., Miki, H., Tezuka, T., Yamamoto, T., Mikoshiba, K. and Takenawa, T.** (2002). Sustained activation of N-WASP through phosphorylation is essential for neurite extension. *Dev. Cell* **3**, 645-658.
- Tarone, G., Cirillo, D., Giancotti, F. G., Comoglio, P. M. and Marchisio, P. C.** (1985). Rous sarcoma virus-transformed fibroblasts adhere primarily at discrete protrusions of the ventral membrane called podosomes. *Exp. Cell Res.* **159**, 141-157.
- Tiffée, J. C., Xing, L., Nilsson, S. and Boyce, B. F.** (1999). Dental abnormalities associated with failure of tooth eruption in src knockout and op/op mice. *Calcif. Tissue Int.* **65**, 53-58.
- van Oijen, M. G., Rijksen, G., ten Broek, F. W. and Slootweg, P. J.** (1998). Overexpression of c-Src in areas of hyperproliferation in head and neck cancer, premalignant lesions and benign mucosal disorders. *J. Oral Pathol. Med.* **27**, 147-152.
- Whitehead, I. P., Campbell, S., Rossman, K. L. and Der, C. J.** (1997). Dbl family proteins. *Biochim. Biophys. Acta* **1332**, F1-F23.
- Xie, X., Chang, S. W., Tatsumoto, T., Chan, A. M. and Miki, T.** (2005). TIM, a Dbl-related protein, regulates cell shape and cytoskeletal organization in a Rho-dependent manner. *Cell. Signal.* **17**, 461-471.
- Yagi, R., Waguri, S., Sumikawa, Y., Nada, S., Oneyama, C., Itami, S., Schmedt, C., Uchiyama, Y. and Okada, M.** (2007). C-terminal Src kinase controls development and maintenance of mouse squamous epithelia. *EMBO J.* **26**, 1234-1244.
- Yamaguchi, H., Lorenz, M., Kempf, S., Sarmiento, C., Coniglio, S., Symons, M., Segall, J., Eddy, R., Miki, H., Takenawa, T. et al.** (2005). Molecular mechanisms of invadopodium formation: the role of the N-WASP-Arp2/3 complex pathway and cofilin. *J. Cell Biol.* **168**, 441-452.
- Yamaguchi, H., Yoshida, S., Muroi, E., Kawamura, M., Kouchi, Z., Nakamura, Y., Sakai, R. and Fukami, K.** (2010). Phosphatidylinositol 4,5-bisphosphate and PIP5-kinase alpha are required for invadopodia formation in human breast cancer cells. *Cancer Sci.* **101**, 1632-1638.
- Yohe, M. E., Rossman, K. and Sondek, J.** (2008). Role of the C-terminal SH3 domain and N-terminal tyrosine phosphorylation in regulation of Tim and related Dbl-family proteins. *Biochemistry* **47**, 6827-6839.
- Zamboni-Zallone, A., Teti, A., Carano, A. and Marchisio, P. C.** (1988). The distribution of podosomes in osteoclasts cultured on bone laminae: effect of retinol. *J. Bone Miner. Res.* **3**, 517-523.

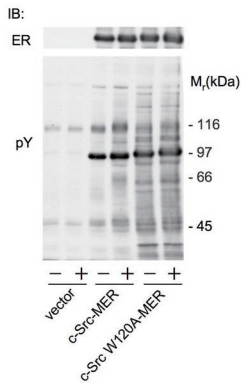
A



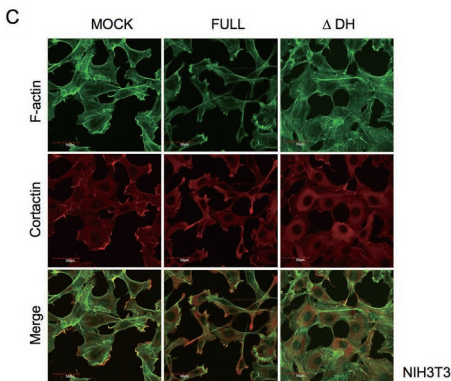
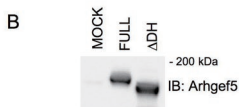
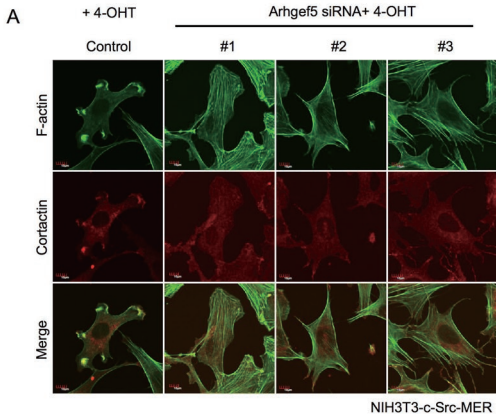
B



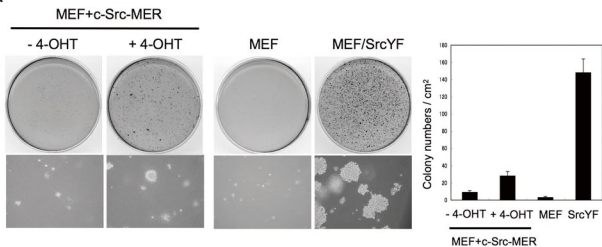
C



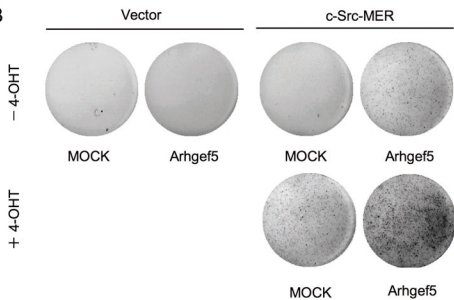
Fraction	Identified Protein	Accession
1	similar to HLA-B associated transcript-2 isoform a isoform 1	XP_538834
2	similar to HLA-B associated transcript-2 isoform a isoform 1	XP_538834
2	similar to rho guanine nucleotide exchange factor 5 isoform 1	XP_539834
2	similar to Cell division cycle 2-related protein kinase 7 (CDC2-related protein kinase 7) (CrkRS) isoform 1	XP_548147
3	similar to Ras association and pleckstrin homology domain 1 isoform 2	XP_545607
4	Splicing factor 3B subunit 1 (Human)	
5	similar to splicing factor 3b, subunit 3 isoform 1	XP_536791
6	similar to splicing factor 3 subunit 1	XP_534733
6	similar to NCK-associated protein 1 isoform 2	XP_535990
6	similar to CBL E3 ubiquitin protein ligase	XP_546487
6	similar to neutrophil cytosolic factor 1	XP_546237
7	similar to Dynamin-2 isoform 3	XP_867900
7	dynamin 1 short form	ACF21009
8	similar to procollagen-lysine, 2-oxoglutarate 5-dioxygenase 3 precursor	XP_858413
9	similar to cyclin K	XP_855304
9	similar to polyadenylate-binding protein 4	XP_857000
10	similar to cleavage and polyadenylation specific factor 6, 68kD subunit	XP_531671
10	similar to polyadenylate-binding protein 1	XP_856590
10	similar to poly(A) binding protein, cytoplasmic	XP_534430
10	similar to Enabled protein homolog	XP_547511
10	similar to heat shock protein 8	XP_850235
11	similar to Wiskott syndrome gene-like protein isoform 1	XP_532445
11	similar to IGF-II mRNA-binding protein 1	XP_548184
12	similar to heterogeneous nuclear ribonucleoprotein K isoform a isoform 6	XP_856705
13	similar to splicing factor 3A subunit 3	XP_849980
14	similar to WIRE protein	XP_850217
14	similar to Tubulin alpha-2 chain	XP_850665
14	vasodilator-stimulated phosphoprotein (VASP)	NP_001003256
14	similar to tubulin, beta, 2	XP_850498
15	vasodilator-stimulated phosphoprotein (VASP)	NP_001003256
15	similar to Elongation factor 1-gamma isoform2	XP_849510
16	similar to heterogeneous nuclear ribonucleoprotein A3 isoform 1	XP_848406
16	similar to 40S ribosomal protein SA	XP_857587
17	similar to suppressor of cytokine signaling 1, protein tyrosine kinase TeclV	
18	CDC42 binding protein kinase beta (Mouse)	
19	similar to cytoplasmic beta-actin isoform 1	XP_536888
20	vasodilator-stimulated phosphoprotein (VASP)	NP_001003256
20	similar to DEAD (Asp-Glu-Ala-Asp) box polypeptide 39 isoform 1	XP_533895
20	BCL-like 2 isoform 4	XP_858803
N1	Keratin	
N2	Keratin	
N3	similar to bromodomain containing protein 3	
N4	similar to heat shock protein 8 isoform 3	
N5	similar to eukaryotic translation elongation factor 1 alpha 1	
N5	similar to Elongation factor 1-gamma isoform 2	
N6	similar to cytoplasmic beta-actin isoform 9	
N6	similar to Actin, cytoplasmic 1 (Beta-actin 1)	



A

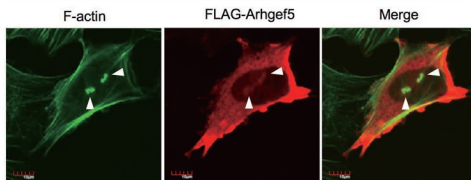


B



A

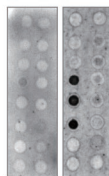
Arhgef5 siRNA + FLAG-Arhgef5 + 4-OHT



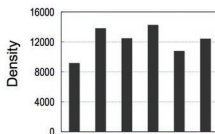
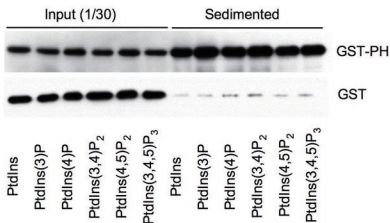
B

NIH3T3-c-*Src*-MER

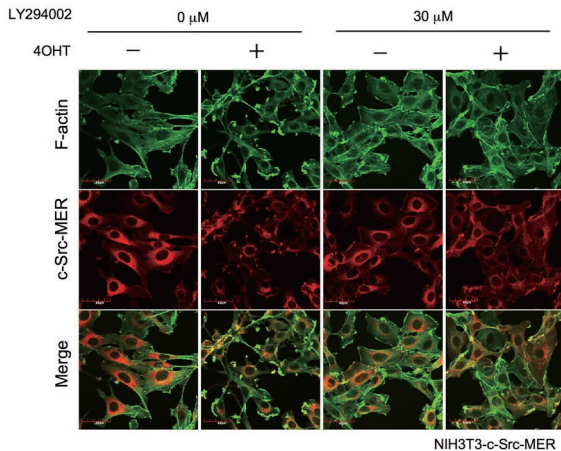
Lysophosphatidic Acid (LPA)	○ ○	Sphingosine-1-phosphate (S1P)
Lysophosphocholine (LPC)	○ ○	PtdIns(3,4)P ₂ (P-3416)
PtdIns (P-0016)	○ ○	PtdIns(3,5)P ₂ (P-3516)
PtdIns(3)P (P-3016)	○ ○	PtdIns(4,5)P ₂ (P-4516)
PtdIns(4)P (P-4016)	○ ○	PtdIns(3,4,5)P ₃ (P-3916)
PtdIns(5)P (P-5016)	○ ○	Phosphatidic Acid PA
Phosphatidylethanolamine PE	○ ○	Phosphatidylserine PS
Phosphatidylcholine PC	○ ○	Blank

GST
GST-PH

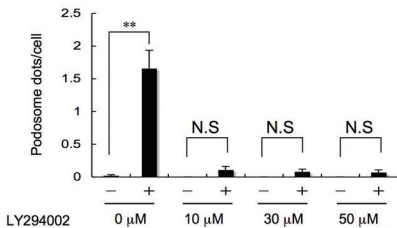
C

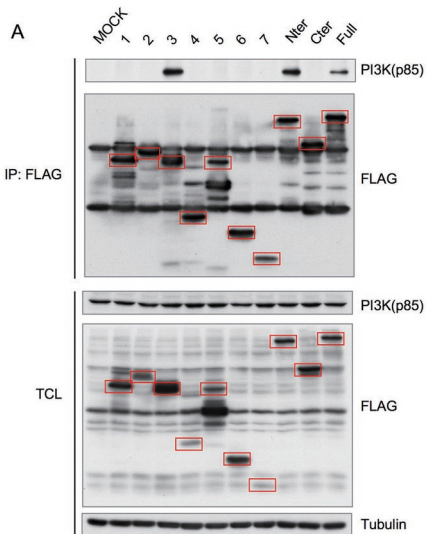


A

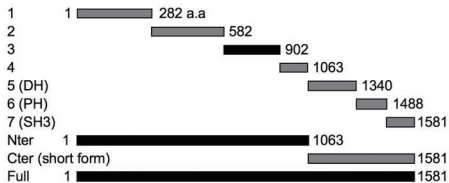


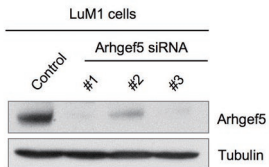
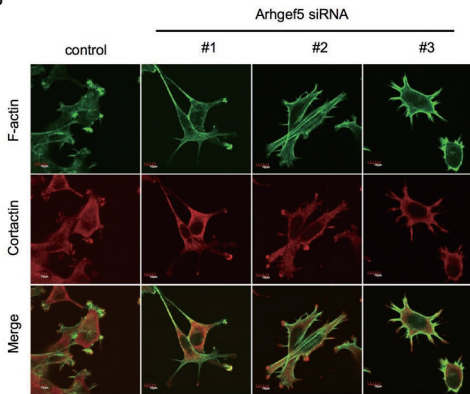
B





B



A**B**

LuM1